Memoir of the Fukui Prefectural Dinosaur Museum 12: 17–33 (2013)

ARTICLE

EVIDENCE FOR LATE PERMIAN–TRIASSIC VOLCANISM IN THE HIDA GAIEN BELT, SOUTHWEST JAPAN： NEW U-PB AGES FROM THE MOTODO, ASHIDANI, AND OTANI FORMATIONS

Yuta KAWAGOE [1] , Norimichi MORI [1] , Shin-ichi SANO [2] , Yuji ORIHASHI [3] , Koshi YAMAMOTO [4] , Yasuo ISHIZAKI [1] , Yoshikazu KOUCHI [1] and Shigeru OTOH [1]

[1] Graduate School of Science and Engineering, University of Toyama, 3190 Gofuku, Toyama 930-8555, Japan
[2] Fukui Prefectural Dinosaur Museum, 51-11 Terao, Muroko, Katsuyama, Fukui 911-8601, Japan
[3] Earthquake Research Institute, University of Tokyo, 1-1-1 Yayoi, Bunkyo-ku, Tokyo 113-0032, Japan
[4] Graduate School of Environmental Studies, Nagoya University, Furo-cho, Chikusa-ku, Nagoya, 464-8601, Japan

ABSTRACT

We carried out a U-Pb geochronological study of the Motodo, Ashidani, and Otani formations in the Hida Gaien Belt of the Kuzuryu area, Fukui Prefecture, in the northeastern part of Southwest Japan, to constrain their age of deposition. The LA-ICPMS U-Pb zircon ages we newly obtained are as follows. Andesitic volcaniclastic conglomerate and tuff breccia of the Lower Member of the Motodo Formation were dated at 254.2 ± 2.5 Ma (2σ) and 253.0 ± 3.6 Ma, respectively. A granodiorite clast of the Middle Member of the formation was dated at 252.6 ± 3.6 Ma. The detrital zircons from the sandstone of the Middle Member of the Motodo Formation and the Ashidani Formation both showed a unimodal age distribution centered at 272–271 Ma. Volcaniclastic sandstone of the Otani Formation showed a multimodal age distribution with peaks at 241 Ma, 433 Ma, 493 Ma, 1720 Ma, and 2409 Ma. Considering the age of tuff breccia and the conformable or interfingering relationship between the members of the Motodo Formation, we interpret that the formation is of Late Permian to Early Triassic age. The youngest age-peak from the volcaniclastic sandstone of the Otani Formation, 243 Ma, presumably indicate the age of syn-sedimentary volcanism, suggesting that the formation is of Middle Triassic age. The Paleoproterozoic zircons in the Otani Formation, on the other hand, indicate the sediment supply from a continent in the Middle Triassic. Combining the new data and the results of previous studies, it is concluded that the Hida Gaien Belt holds evidence for continual volcanism from the Ordovician to the Late Triassic.

Key words: U-Pb age, zircon, LA-ICPMS, Hida Gaien Belt, Fukui Prefecture

川越雄太・森　紀道・佐野晋一・折橋裕二・山本鋼志・石崎泰男・高地吉一・大藤　茂（2013）西南日本，飛騨外縁帯の本戸層，芦谷層および大谷層から得られた新たな LA-ICPMS ウラン－鉛年代．福井県立恐竜博物館紀要 12：17–33.

飛騨外縁帯，本戸層，芦谷層及び大谷層のウラン－鉛ジルコン年代を検討した．本戸層下部層の火砕性礫岩及び凝灰角礫岩の年代は，それぞれ 254.2 ± 2.5 Ma（2 σ）及び 253.0 ± 3.6 Ma である．また，同層中部層の花崗閃緑岩礫の年代は 252.6 ± 3.6 Ma である．本戸層中部層及び芦谷層の砂岩中の砕屑性ジルコンは，272–271 Ma をピークとする単峰型年代分布をなす．大谷層の火砕性砂岩中の砕屑性ジルコンは，243 Ma，493 Ma，1720 Ma，2409 Ma 等の多峰型年代分布をなす．本戸層は，上記データ及び各部層の整合・指交関係から，上部ペルム～下部三畳系と解釈される．大谷層は，火砕性砂岩中の最も若い年代ピークが堆積時火山活動を示す蓋然性が高く，中部三畳系と推定される．また，大谷層中の古原生代の年代は，大陸からのジルコン供給の開始を示唆する．新たなデータと先行研究より，飛騨外縁帯はオルドビス紀～後期三畳紀の断続的な火山活動を記録することが判明した．

Received August 5, 2013. Accepted November 14, 2013.
Corresponding author—Shigeru OTOH
E-mail: shige@sci.u-toyama.ac.jp

INTRODUCTION

The Hida Gaien (or Marginal) Belt is the tectonic belt between the Hida and Oeyama or Renge belts of the Inner Zone of Southwest Japan, and consists mainly of Middle to Upper Paleozoic and Upper Triassic shallow marine beds (Tsukada et al., 2004; Fig. 1). The constituent rocks of the Hida Gaien Belt sporadically occur in the Omi–Shirouma, Fukuji–Takayama, Naradani, and Kuzuryu areas in the northeastern part of Southwest Japan (Fig. 1). The belt has been famous for the occurrence of Paleozoic, especially Middle Paleozoic mega- and microfossils since the early twentieth century (e.g., Kozu, 1910; Kato, 1913; Kamei, 1952; Igo, 1956; Kawai et al., 1957; Hamada, 1959; Kato, 1959; Igo et al., 1980; Tsukada and Koike, 1997; Kurihara, 2004).

The Hida Gaien Belt is also characterized by the abundance of volcanic, pyroclastic, and volcaniclastic rocks, which have been well dated in the Fukuji–Takayama area. Ordovician or older mafic volcanism is recorded in the Iwatsubodani Formation (Tsukada, 1997), Ordovician–Silurian felsic volcanism in the Hitoegane Formation (Tsukada and Koike, 1997; Tsukada, 1997), Devonian felsic volcanism in the Yoshiki Formation (Kurihara, 2004), Carboniferous mafic and felsic volcanism in the Arakigawa Formation (Isomi and Nozawa, 1957), Early–Middle Permian felsic volcanism in the Mizuyagadani Formation (Niko et al., 1987), Middle Permian mafic to intermediate volcanism in the Sorayama Formation (Tsukada et al., 1999; Tsukada and Takahashi, 2000), and Late Triassic felsic to intermediate volcanism in the Tandodani Formation (Tsukada et al., 1997; Tsukada and Niwa, 2005). Volcanic and related rocks are also abundant in the Kuzuryu area of the Hida Gaien Belt: e.g., in the Kagero, Shibasudani, Konogidani, Tomedoro, Motodo, and Otani formations as described in a later section. Although the ages of the Kagero and Shibasudani formations have been determined by radiolarian biostratigraphy as Early Silurian and Late Silurian–Devonian, respectively (Kurihara, 2003, 2004), and Late Cretaceous K-Ar and Ar-Ar plagioclase ages were reported from the Konogidani Formation (Matsumoto, 2012b), many age-unknown formations have remained. The insufficiency of biostratigraphical and geochronological data impedes the full understanding of the geologic development of Southwest Japan.

In this paper, we report newly obtained LA-ICPMS (laser ablation inductively coupled plasma mass spectrometry), U-Pb zircon ages from the Motodo, Ashidani, and Otani formations in the northern part of the Kuzuryu area, Hida Gaien Belt. As will be discussed later, the data suggests that these formations are of Late Permian or Triassic age, quite discordant with the major opinion that correlates the Motodo Formation with the Lower Cretaceous Kanmon Group in western Southwest Japan. Hence we compare the detrital zircon age distributions of the Motodo Formation and Hayama Formation, which is correlated with the Kanmon Group, as a control test. Finally we discuss the tectonic setting of the Late Permian–Triassic volcanism recorded in the Motodo and Otani formations.

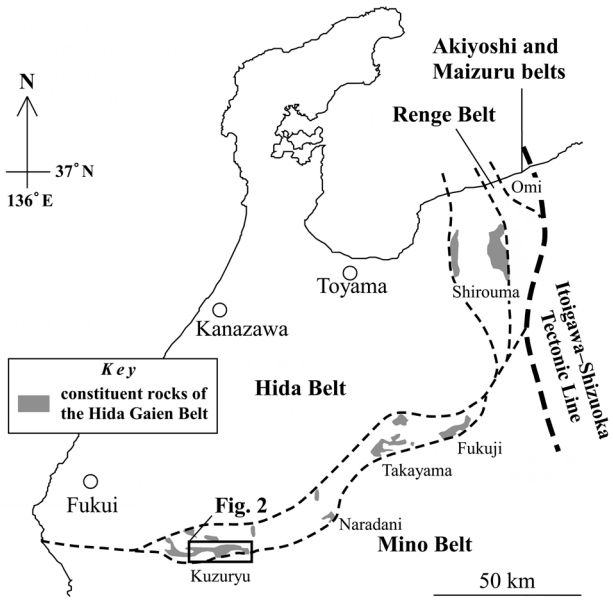

FIGURE 1. Index map showing the distribution of the constituent rocks of the Hida Gaien Belt and the location of the Kuzuryu area drawn in Fig. 2. Modified after Tsukada et al. (2004).

GEOLOGIC SETTING

Kuzuryu area of the Hida Gaien Belt

The Kuzuryu area lies in the southwestern part of the Hida Gaien Belt. The constituent rocks of the Hida Gaien Belt widely occur in the area and have been studied by many researchers (e.g., Kawai et al., 1957; Maeda, 1961; Kurihara, 2003; Otoh et al., 2004; Fukui Prefecture, 2010; Matsumoto, 2012b). The Kuzuryu area is mainly occupied by the following geologic units: the Ise Metamorphic Rocks of the Renge Belt metamorphosed in Late Carboniferous–Early Permian age (Kunugiza et al., 2004), Lower Silurian Kagero Formation, Upper Silurian–Lower Devonian Shibasudani Formation, Lower Devonian Kamianama Formation, Carboniferous Fujikuradani Formation, Upper Carboniferous Nagano Formation, Middle Permian Oguradani Formation, Upper Cretaceous Konogidani Formation, age-unknown Tomedoro, Motodo, Ashidani and Otani formations, and Middle Jurassic–Lower Cretaceous Tetori Group (Fig. 2). Among them, we studied the age-unknown Motodo, Ashidani, and Otani formations. Here we introduce the outline of the three formations.

Motodo Formation

The Motodo Formation (Kobayashi, 1954; Yamada, 1967) extends eastward from the type locality, some 20 km to the west of the Kuzuryu Dam, to the south of Otani (Kawai et al., 1957; submerged in Lake Kuzuryu-ko at present; Fig. 2). There are also narrow exposures of the formation near the upper stream of the Konogidani Valley. The formation strikes east to ENE and dips 30°–60°S, quite discordant with the geologic structure of

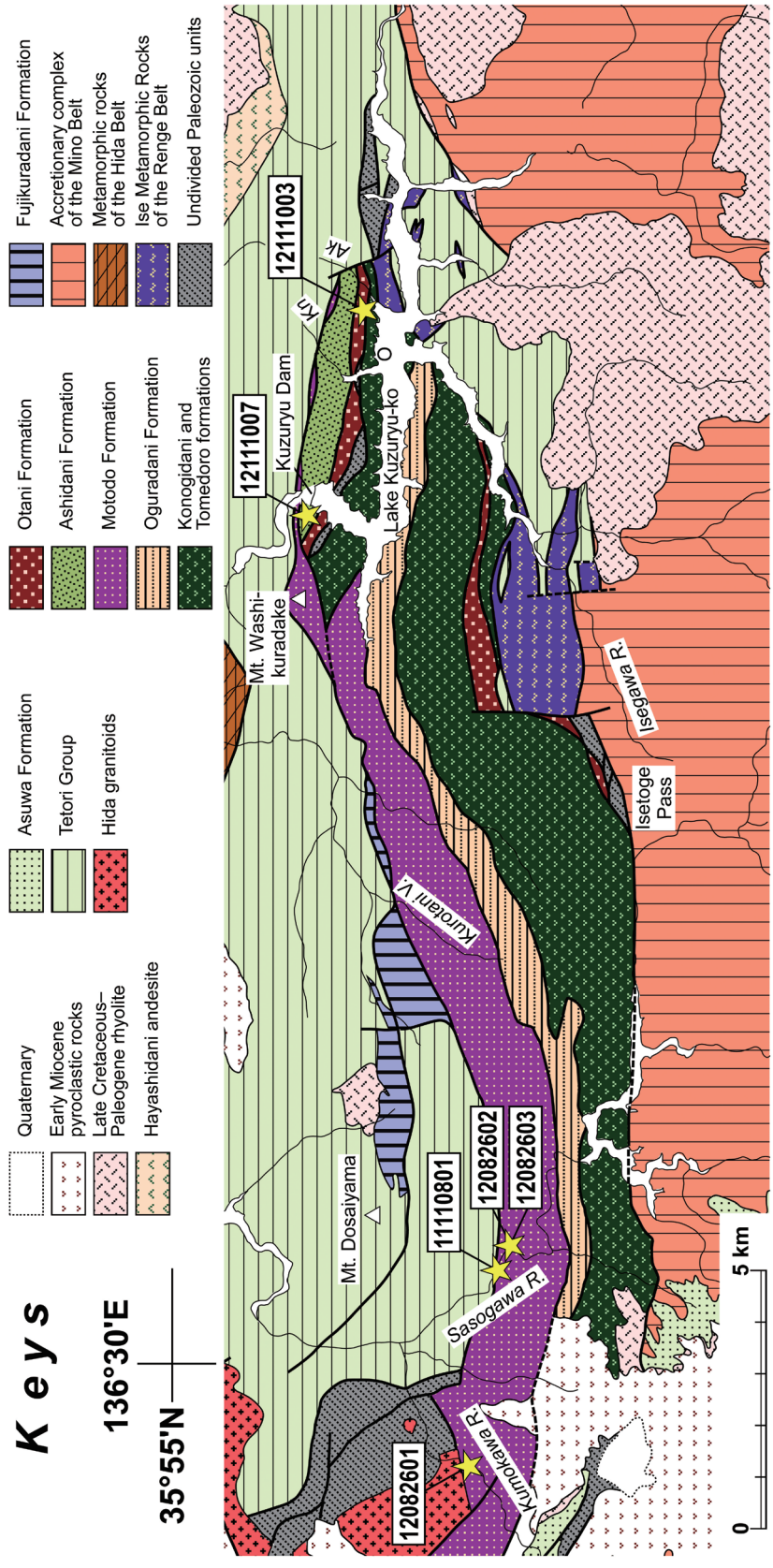

FIGURE 2. Geologic map of the Kuzuryu area showing the sampling locations. Compiled from Otoh et al. (2004), Fukui Prefecture (2010), and Matsumoto (2012b). Abbreviations—*Ak*: Akubaradani Valley, *Kn*: Konogidani Valley, O: Otani, R.: River, V.: Valley.

the Tetori Group that dips and faces to the north. The Motodo Formation consists of the Nakajima Tuff Breccia, Wasadani Conglomerate, and Kumokawa Conglomerate members, in ascending order (Ono and Takeuchi, 2001). The Wasadani Conglomerate Member conformably covers the Nakajima Tuff Breccia Member, whereas the Kumokawa Conglomerate Member conformably covers or interfingers with the Wasadani Conglomerate Member. The total thickness of the formation exceeds 1,000 m (Ono and Takeuchi, 2001; Matsumoto, 2012b).

The Nakajima Tuff Breccia Member consists of andesitic tuff breccia and volcanic breccia with blocks and lapillis of andesite lava and pyroclastic rocks contained in the matrix of lithic tuff (Ono and Takeuchi, 2001). The tuff breccia and volcanic breccia rarely contain pebble- to cobble-sized limestone clasts that yield Middle Permian fusulinids such as *Lepidolina toriyamai* (Omura, 1968).

The Wasadani Conglomerate Member consists mainly of matrix-supported, ill-sorted massive conglomerate and dark green or reddish purple sandstone. The conglomerate is composed of pebbles to boulders of granitoids, felsic volcanic rocks, limestone, and mafic volcanic rocks contained in the matrix of dark green to dark gray coarse sandstone. The clasts of granitoids and felsic volcanic rocks tend to be larger and better-rounded, whereas those of the other rock types tend to be smaller and worse-rounded. Ono et al. (2003) reported CHIME zircon ages of 201 ± 20 Ma and 202 ± 30 Ma (Late Triassic–Early Jurassic) from granodiorite pebbles of the member.

The Kumokawa Conglomerate Member consists mainly of clast-supported, moderately- to ill-sorted, bedded reddish purple conglomerate and reddish purple sandstone. The conglomerate is composed mainly of pebbles and cobbles of reddish purple sandstone and mudstone, along with rare limestone clasts (Ono and Takeuchi, 2001). The limestone clasts yield Middle to Late Permian fusulinids such as *Codonofusiella* sp., *Reichelina* sp., and *Yangchienia* sp. (Omura, 1968).

The data set as well as the lithological resemblance (dominance of red beds) has become a strong basis to believe that the Motodo Formation is correlated with the Lower Cretaceous Kenseki Formation or Kanmon Group in the western part of Southwest Japan (Kobayashi, 1954; Kawai et al., 1957; Ono et al., 2003; Matsumoto, 2012b). Omura (1968), on the other hand, proposed that the Motodo Formation is an Upper Permian to Triassic formation from the following reasons: (1) the Motodo Formation yielded no Mesozoic fossils; (2) the Motodo Formation, dipping steeply to south along with the Paleozoic formations, was presumably older than the Middle Jurassic to Lower Cretaceous Tetori Group, which dipped gently to north; (3) the paleomagnetic poles of the Motodo Formation and Kanmon Group differed from each other.

Ashidani Formation

The Ashidani Formation (Kawai, 1956) extends eastward from the type locality on the east of the Kuzuryu Dam to the upper stream of the Akubaradani Valley (Fig. 2). The formation strikes WNW to ENE, dips 60°–90°S, and apparently overlies the Motodo Formation near the upper stream of the Konogidani Valley. The apparent thickness of the formation is 1,000 m. The Ashidani Formation consists of greenish gray, medium- to coarse-grained sandstone and black mudstone, with a thin layer of conglomerate and lenticular limestone bodies. The formation has been strongly sheared and exhibits distinct schistosity and lineation. The schistosity is defined by parallel arrangement of the (001) plane of micas and/or the xy-plane of stretched sand grains ($x > y > z$), and is parallel to the bedding plane. The lineation defined by parallel arrangement of the x-axis of stretched sand grains lies on the schistosity and gently plunges to west or east. A lenticular limestone body near the type locality yields Late Carboniferous fusulinids such as *Fusulinella pseudobocki* (Kobayashi, 1954). Matsumoto (2012a) reported SHRIMP U-Pb ages of detrital zircons from the Ashidani Formation. He found that the age of detrital zircons ranges between 280 Ma and 220 Ma and inferred that the Ashidani Formation is a Triassic formation.

Otani Formation

The Otani Formaiton (Yamada, 1967) shows east-trending, long and narrow distribution around the type locality at Otani, along the lower stream of the Konogidani Valley (Fig. 2). The formation strikes east and dips 60°–90°S. The apparent thickness of the formation near the type locality exceeds 500 m. The formation also occurs to the south of Lake Kuzuryu-ko (Fig. 2). The Otani Formation consists of conglomerates with the dark green to dark brown matrix of altered andesitic to basaltic volcaniclastic sandstone. The conglomerate is very ill-sorted, containing grains of various sizes ranging from 0.5 mm to 70 cm, and is rounded to sub-angular. Moreover there are some mappable blocks (mainly of limestone) with the longest dimension of up to several hundred meters. According to Matsumoto (2012b), the clast composition of the conglomerate in an outcrop on the left bank of the Konogidani Valley was andesite (33%), basalt (24%), limestone (15%), granite (9%), rhyolite (7%), and gabbro (6%), in descending order. The limestone pebbles yield a coral fossil *Favosites* sp., and fusulinids such as *Fusulinella* sp., *Triticites* sp., *Obsoletes* sp., *Schubertella kingi*, *Schwagerina japonica*, and *Lepidolina kumaensis* (Kawai et al., 1957; Yamaguchi and Ota, 1965; Yamada, 1967; Matsumoto, 2012b). In addition, the Metal Mining Agency of Japan (1980) reported whole rock K-Ar age of 159.3 ± 8.0 Ma from an andesite pebble of the Otani Formation near Loc. 12111003 (Ichinomata bridge; Matsumoto, 2012b).

Nariwa area of the Akiyoshi Belt, Okayama Prefecture

The Nariwa area lies in the southern part of the Akiyoshi Belt in the eastern Chugoku Mountains, Southwest Japan (Fig. 3). The Nariwa area consists mainly of the Permian accretionary complex of the Akiyoshi Belt, composed of Carboniferous to Middle Permian reef limestone and chert and Middle Permian terrigenous clastic rocks and felsic tuff (e.g., Sano et al., 1987). The Upper Triassic shallow marine to terrestrial clastic rocks of the Nariwa Group unconformably overlies the accretionary complex (Otoh, 1985), and the Lower Cretaceous fluvial

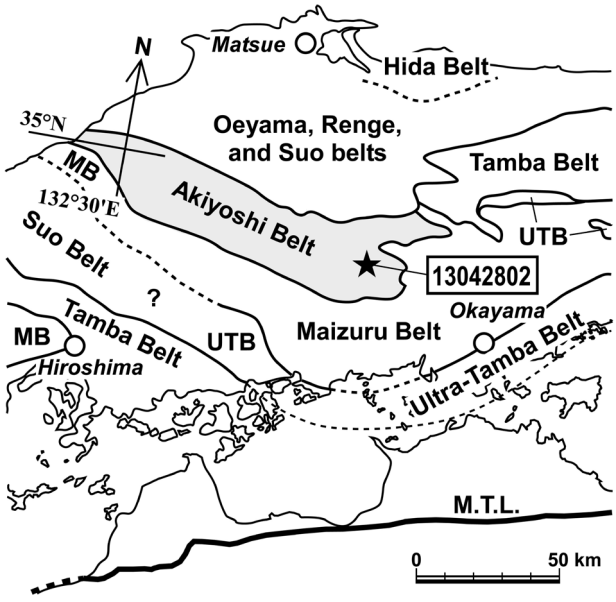

FIGURE 3. Simplified tectonic map of the eastern Chugoku Mountains showing the sampling location of the Hayama sandstone (sample 13042802). Abbreviations—MB: Maizuru Belt, M.T.L.: Median Tectonic Line, UTB: Ultra-Tamba Belt.

deposits of the Hayama Formation unconformably overlies them (Suzuki et al., 2001).

Hayama Formation

The Hayama Formation (Suzuki et al., 2001), 300 m thick, occurs in the northwestern part of the Nariwa Town, Takahashi City, Okayama Prefecture. The formation was called the Kenseki (or Inkstone) Formation (Kusumi et al., 1965) in the twentieth century. The Hayama Formation consists characteristically of upward fining red fluvial clastic rocks and is divided into two members: the Eda Conglomerate Member and Sora Mudstone Member, in ascending order (Suzuki et al., 2001). The Eda Conglomerate Member consists mainly of limestone conglomerate with minor clasts of chert, sandstone, and felsic tuff, and is associated with red sandstone layers. The Sora Mudstone Member consists mainly of red to reddish purple mudstone, interlayered with red sandstone. Suzuki et al. (2001) obtained a fission track age of 101 ± 4 Ma from zircons in a felsic tuff layer of the Sora Mudstone Member and concluded that the Hayama Formation is correlated with the Aptian Shimonoseki Subgroup of the Kanmon Group in the western part of Southwest Japan.

SAMPLE DESCRIPTIONS

We studied the following six samples and constrained their age of deposition: (1) andesitic volcaniclastic conglomerate of the Motodo Formation, (2) andesitic tuff breccia of the Nakajima Tuff Breccia Member of the Motodo Formation, (3) a granodiorite cobble of the Wasadani Conglomerate Member of the Motodo Formation, (4) a sandstone matrix of the Wasadani Conglomerate Member containing the above granodiorite cobble, (5) sandstone of the Ashidani Formation, and (6) granule sandstone of the Otani Formation. In addition, we carried out a preliminary study of (7) red sandstone of the Hayama Formation. Here follow the description of the samples studied.

Andesitic volcaniclastic conglomerate of the Nakajima Tuff Breccia Member (Sample 11110801; N35°51'33.1", E136°31'22.7")

Sample 11110801 of the Nakajima Tuff Breccia Member of the Motodo Formation was collected from an exposure of the lowermost part of the member along the middle stream of the Sasogawa River (Fig. 2). The sample was of volcaniclastic conglomerate with pebble- to cobble-sized clasts of andesite lava, andesitic lapilli tuff, and felsic vitric tuff contained in the matrix of dark reddish purple andesitic tuff to lapilli tuff. The conglomerate is ill-sorted, subangular to moderately rounded, and matrix supported. We crushed the clasts and matrix of the conglomerate together and collected zircon grains. The zircon grains were mostly euhedral and colorless, with some brown grains. They had columnar shapes with the aspect ratio ranging from 1.3 to 2.8 (1.7 in average). All zircon grains showed oscillatory zoning in cathodoluminescence (CL) images, a common feature of igneous zircons (Corfu et al., 2003).

Andesitic tuff breccia of the Nakajima Tuff Breccia Member (Sample 12082601; N35°51' 53.8", E136°28' 52.6")

Sample 12082601 of the Nakajima Tuff Breccia Member of the Motodo Formation was collected from an exposure of the lower part of the member along the Kumokawa River (Fig. 2). The sample was of tuff breccia consisting of clasts of andesite lava and felsic vitric tuff contained in the matrix of dark purple lithic lapilli tuff. We did not separate the clasts and matrix, crushed them together, and collected zircon grains. The zircon grains were euhedral to subhedral and colorless. They had columnar shapes with the aspect ratio of around 2.5. All zircon grains showed oscillatory zoning in CL images.

Granodiorite cobble of the Wasadani Conglomerate Member (Sample 12082602; N35°51'25.2", E136°31'40.2")

Sample 12082602 of the Wasadani Conglomerate Member of the Motodo Formation was collected from an exposure of conglomerate of the lower part of the member along the Sasogawa River (Fig. 2). The sample was a granodiorite cobble comprising plagioclase (47%; partly saussuritized and/or sericitized), quartz (22%), biotite (19%; partly chloritized), and pink K-feldspar (12%). The volume ratio of quartz, plagioclase, and K-feldspar was 27 : 58 : 15. The zircon grains we collected were euhedral to subhedral and colorless. They had columnar shapes with the aspect ratio ranging from 1.6 to 2.8 (mostly 2.5). All zircon grains showed oscillatory zoning in CL images.

Sandstone of the Wasadani Conglomerate Member (Sample 12082603; N35°51'25.2", E136°31'40.2")

Sample 12082603 of the Wasadani Conglomerate Member of the Motodo Formation was collected from the same exposure with sample 12082602 (Fig. 2). The sample was of feldspathic arenite composing the matrix of conglomerate, and consisted of feldspars (50%; partly saussuritized and/or sericitized), rock fragments (21%), single quartz (20%), and matrix (9%). The zircon grains we collected were mostly subhedral to anhedral and colorless, with rare brown grains. They had columnar shapes with the aspect ratio ranging from 1.6 to 3.2 (2.3 in average). All zircon grains showed oscillatory zoning in CL images.

Sandstone of the Ashidani Formation (Sample 12111007; N35°53'21.6", E136°40'48.8")

Sample 12111007 of the Ashidani Formation was collected from an exposure along a logging road to the east of Mt. Washikuradake (Fig. 2). The sample was of bedded lithic arenite in the upper part of the formation, containing lithic fragments of mudstone, felsic volcanic rocks, and chert. The sandstone was ill- to moderately-sorted, sub-angular and had undergone cataclastic deformation. The zircon grains we collected were mostly euhedral to subhedral and colorless, with rare brown grains. They had columnar shapes with the aspect ratio ranging from 1.6 to 3.0 (2.4 in average). All zircon grains showed oscillatory zoning in CL images.

Sandstone of the Otani Formation (Sample 12111003; N35°52'49.2", E136°43'39.5")

Sample 12111003 of the Otani Formation was collected from an exposure along a branch of the Akubaradani Valley to the north of the Ichinomata bridge (Fig. 2). The sample was of volcaniclastic sandstone–granule conglomerate composing the matrix of ill-sorted conglomerate of the Otani Formation. The sample consisted mostly of subangular fragments of altered andesitic volcanic rocks with minor single quartz and feldspar grains. The zircon grains we collected were mostly euhedral and colorless, with rare brown grains. They had columnar shapes with the aspect ratio ranging from 1.4 to 2.7 (2.0 in average). All zircon grains showed oscillatory zoning in CL images.

Sandstone of the Hayama Formation (Sample 13042802; N34°47'58.4", E133°30'45.8")

Sample 13042802 of the Hayama Formation was collected from the lower part of the formation (Eda Conglomerate Member), at an exposure along the middle stream of the Shimagigawa River to the northwest of Nariwa Town, Takahashi City, Okayama Prefecture (Fig. 3). The sample was of bedded lithic arenite intercalated in thick red conglomerate beds of the Eda Conglomerate Member. The sample consisted of lithic fragments (60%), feldspar (20%), quartz (13%), and matrix (7%). The lithic fragments were mainly of felsic volcanic rocks. The zircon grains we collected were mostly euhedral and colorless, with rare brown grains. They had columnar shapes with the aspect ratio ranging from 1.5 to 3.0 (2.4 in average). All zircon grains showed oscillatory zoning in CL images.

ANALYTICAL METHOD

The zircon samples for analyses were prepared in accordance with the procedures described in Kawagoe et al. (2012). The measurement was carried out on laser ablation inductively coupled plasma mass spectrometers (LA-ICPMS) equipped in the (1) Earthquake Research Institute of the University of Tokyo (ERI), and (2) Graduate School of Environmental Studies, Nagoya University (NU).

The ICPMS instrument equipped in ERI was a Thermo Elemental Plasma Quad 3 quadropole-based ICPMS connected with a New Wave UP-213 LA system, which used the frequency quintupled Nd-YAG 213-nm wavelength (Orihashi et al., 2008). The measurement conditions were as follows: the ablation pit size of 30 μm, energy density of 11–13 J/cm^{-2}, and pulse repetition rate of 10 Hz. The analyses were carried out in a peak-jumping mode and the peaks of ^{202}Hg, ^{206}Pb, ^{207}Pb, ^{208}Pb, ^{232}Th, and ^{238}U were monitored. Data were acquired in sequences of 28 analyses, consisting of 5 analyses of gas blank, 4 NIST (National Institute of Standards and Technology, U.S.A.) SRM 610 glass standard, 1 standard zircon (91500 zircon with the ^{206}Pb/^{238}U age of 1062.4 ± 0.4 Ma; Wiedenbeck et al., 1995), 9 unknown, 4 SRM 610 standard, and 5 gas blank.

The ICPMS instrument equipped in NU was an Agilent 7700x quadropole-based ICPMS connected with a New Wave Research NWR-213-type LA system, which used the frequency quintupled Nd-YAG 213-nm wavelength. The measurement conditions, optimized to reduce matrix effects, were as follows: energy density of 11.7 J/cm^{-2}, pulse repetition rate of 10 Hz, pre-ablation time of 8 s, ablation time of 10 s, and the ablation pit size of 25 μm (Kouchi et al., 2012). The analyses were carried out in a peak-jumping mode and the peaks of ^{202}Hg, ^{206}Pb, ^{207}Pb, ^{208}Pb, ^{232}Th, and ^{238}U were monitored. Data were acquired in the same sequences with the ERI system.

RESULTS

We sampled an outer part (rim or mantle) of collected zircon grains with the laser ablation technique, and analyzed with the ICPMS. After the analyses we processed the data with the Microsoft Excel and Isoplot 3.70 softwares (Ludwig, 2008) and drew various diagrams shown in this paper. Here follow the results of our analyses (Table 1).

TABLE 1. U-Pb isotopic data for zircons analyzed in this study. All errors are 2σ. % conc = 100•($^{206}Pb/^{238}U$ age)/($^{207}Pb/^{235}U$ age) is a measure of concordance between $^{206}Pb/^{238}U$ and $^{207}Pb/^{235}U$ ages. Analyses shown in italics are discordant ones that are not included in the probability density plot and histogram. Abbreviation—Cgl.: Conglomerate.

Grain	$^{206}Pb/^{238}U$	$^{207}Pb/^{235}U$	$^{206}Pb/^{238}U$ age (Ma)	$^{207}Pb/^{235}U$ age (Ma)	% conc	Th/U
Nakajima Tuff Breccia Member: Andesitic Volcaniclastic Cgl. (11110801; N35°51'33.1", E136°31'22.7")						
NT-1.1	0.0405 ± 0.0012	0.294 ± 0.010	255.7 ± 7.5	261.5 ± 8.9	97.8	0.46
NT-1.2	0.0400 ± 0.0012	0.292 ± 0.012	252.6 ± 7.5	260 ± 11	97.0	1.80
NT-1.3	0.0413 ± 0.0012	0.299 ± 0.013	260.6 ± 7.8	265 ± 11	98.2	2.43
NT-1.4	0.0398 ± 0.0012	0.302 ± 0.013	251.5 ± 7.5	268 ± 12	93.8	0.56
NT-1.5	0.0403 ± 0.0012	0.299 ± 0.012	254.7 ± 7.6	265 ± 11	96.0	0.44
NT-1.6	0.0397 ± 0.0015	0.301 ± 0.015	250.7 ± 9.8	268 ± 13	93.7	0.54
NT-1.7	0.0394 ± 0.0015	0.304 ± 0.016	249.2 ± 9.7	269 ± 14	92.5	0.60
NT-1.8	0.0403 ± 0.0016	0.295 ± 0.016	255 ± 10	262 ± 14	97.2	0.57
NT-1.9	0.0391 ± 0.0015	0.288 ± 0.013	247.3 ± 9.6	257 ± 12	96.3	0.61
NT-1.10	0.0398 ± 0.0015	0.286 ± 0.013	251.9 ± 9.8	255 ± 12	98.7	0.67
NT-1.11	0.0414 ± 0.0016	0.303 ± 0.013	261 ± 10	269 ± 12	97.3	0.47
NT-1.12	0.0409 ± 0.0016	0.310 ± 0.017	259 ± 10	274 ± 15	94.4	0.93
Nakajima Tuff Breccia Member: Andesitic Tuff Breccia (12080601; N35°51'53.8", E136°28'52.6")						
NT-2.1	0.0434 ± 0.0013	0.310 ± 0.040	273.9 ± 7.9	274 ± 35	100.0	0.40
NT-2.2	0.04345 ± 0.00082	0.290 ± 0.016	274.2 ± 5.2	259 ± 14	106.1	0.63
NT-2.3	0.04341 ± 0.00088	0.308 ± 0.020	274.0 ± 5.5	273 ± 18	100.4	1.05
NT-2.4	0.04324 ± 0.00080	0.317 ± 0.016	272.9 ± 5.0	280 ± 14	97.5	0.77
NT-2.5	0.04081 ± 0.00098	0.292 ± 0.027	257.8 ± 6.2	260 ± 24	99.2	0.48
NT-2.6	0.0434 ± 0.0010	0.307 ± 0.029	273.7 ± 6.6	272 ± 25	100.8	0.71
NT-2.7	0.0440 ± 0.0010	0.376 ± 0.030	277.7 ± 6.5	324 ± 26	85.7	0.68
NT-2.8	0.0425 ± 0.0012	0.280 ± 0.037	268.2 ± 7.7	250 ± 33	107.1	0.40
NT-2.9	0.0400 ± 0.0012	0.306 ± 0.031	253.1 ± 7.5	271 ± 27	93.5	0.80
NT-2.10	0.03929 ± 0.00094	0.277 ± 0.012	248.4 ± 5.9	249 ± 11	99.9	0.58
NT-2.11	0.0440 ± 0.0012	0.342 ± 0.026	277.6 ± 7.6	299 ± 23	92.9	0.63
NT-2.12	0.0443 ± 0.0014	0.313 ± 0.037	279.5 ± 8.6	276 ± 33	101.1	0.71
NT-2.13	0.0444 ± 0.0011	0.358 ± 0.016	280.4 ± 6.8	311 ± 14	90.3	0.70
NT-2.14	0.0435 ± 0.0015	0.326 ± 0.046	274.4 ± 9.2	287 ± 41	95.8	0.44
Wasadani Conglomerate Member: Granodiorite Cobble (12080602; N35°51'25.2", E136°31'40.2")						
WC g-1.1	0.03874 ± 0.00094	0.280 ± 0.017	245.0 ± 6.0	251 ± 15	97.7	1.18
WC g-1.2	0.04059 ± 0.00096	0.284 ± 0.015	256.5 ± 6.1	254 ± 13	101.0	1.48
WC g-1.3	0.0410 ± 0.0010	0.296 ± 0.018	258.8 ± 6.3	263 ± 16	98.3	1.20
WC g-1.4	0.04176 ± 0.00098	0.298 ± 0.015	263.7 ± 6.2	265 ± 13	99.6	1.31
WC g-1.5	0.0403 ± 0.0011	0.271 ± 0.023	254.7 ± 6.8	244 ± 21	104.5	1.12
WC g-1.6	0.0405 ± 0.0010	0.274 ± 0.020	255.7 ± 6.5	246 ± 18	104.0	1.11
WC g-1.7	0.04029 ± 0.00095	0.332 ± 0.016	254.6 ± 6.0	291 ± 14	87.5	1.00
WC g-1.8	0.0402 ± 0.0010	0.331 ± 0.022	254.3 ± 6.5	290 ± 19	87.6	1.02
WC g-1.9	0.04013 ± 0.00076	0.291 ± 0.013	253.6 ± 4.8	259 ± 12	97.9	1.42
WC g-1.10	0.04016 ± 0.00084	0.284 ± 0.017	253.8 ± 5.3	254 ± 15	100.1	1.32
WC g-1.11	0.04004 ± 0.00077	0.295 ± 0.014	253.1 ± 4.9	262 ± 12	96.5	1.53
WC g-1.12	0.03910 ± 0.00080	0.301 ± 0.017	247.2 ± 5.0	267 ± 15	92.6	1.21
WC g-1.13	0.03842 ± 0.00082	0.290 ± 0.018	243.1 ± 5.2	259 ± 16	93.9	1.18
WC g-1.14	0.04000 ± 0.00087	0.315 ± 0.020	252.8 ± 5.5	278 ± 18	90.8	1.04

Grain	$^{206}Pb/^{238}U$	$^{207}Pb/^{235}U$	$^{206}Pb/^{238}U$ age (Ma)	$^{207}Pb/^{235}U$ age (Ma)	% conc	Th/U
Wasadani Conglomerate Member: Sandstone (12080603; N35°51'25.2", E136°31'40.2")						
WC ss-1.1	0.0436 ± 0.0017	0.301 ± 0.041	275 ± 11	267 ± 36	97.2	0.70
WC ss-1.2	0.0442 ± 0.0020	0.345 ± 0.054	279 ± 12	301 ± 47	107.9	0.67
WC ss-1.3	0.0434 ± 0.0015	0.311 ± 0.033	273.9 ± 9.6	275 ± 29	100.5	0.63
WC ss-1.4	0.0441 ± 0.0019	0.326 ± 0.050	278 ± 12	286 ± 44	102.8	0.54
WC ss-1.5	0.0411 ± 0.0013	0.316 ± 0.024	259.4 ± 8.1	279 ± 21	107.4	1.64
WC ss-1.6	0.0415 ± 0.0015	0.306 ± 0.033	262.2 ± 9.4	271 ± 30	103.4	0.56
WC ss-1.7	0.0431 ± 0.0017	0.295 ± 0.042	272 ± 11	263 ± 37	96.5	0.65
WC ss-1.8	0.0457 ± 0.0013	0.345 ± 0.034	288.0 ± 7.9	301 ± 30	104.5	0.53
WC ss-1.9	0.0434 ± 0.0011	0.311 ± 0.027	273.6 ± 6.9	275 ± 24	100.5	0.71
WC ss-1.10	0.0429 ± 0.0010	0.327 ± 0.026	270.8 ± 6.5	287 ± 23	106.0	1.13
WC ss-1.11	0.0441 ± 0.0016	0.329 ± 0.049	278 ± 10	289 ± 43	103.8	0.61
WC ss-1.12	0.0438 ± 0.0014	0.312 ± 0.041	276.2 ± 9.1	275 ± 36	99.7	0.47
WC ss-1.13	0.0419 ± 0.0010	0.286 ± 0.023	264.3 ± 6.3	255 ± 21	96.6	0.90
WC ss-1.14	0.0445 ± 0.0015	0.332 ± 0.044	280.9 ± 9.6	291 ± 39	103.7	0.67
WC ss-1.15	0.0426 ± 0.0011	0.314 ± 0.028	268.6 ± 6.9	277 ± 24	103.1	1.12
WC ss-1.16	0.0433 ± 0.0014	0.307 ± 0.040	273.3 ± 8.9	272 ± 36	99.4	0.62
WC ss-1.17	0.0422 ± 0.0014	0.299 ± 0.039	266.4 ± 8.6	266 ± 34	99.8	0.67
WC ss-1.18	*0.0452 ± 0.0015*	*0.389 ± 0.048*	*285.1 ± 9.4*	*334 ± 41*	*117.0*	*0.74*
WC ss-1.19	0.0416 ± 0.0015	0.274 ± 0.042	262.6 ± 9.4	246 ± 37	93.6	0.50
WC ss-1.20	0.0430 ± 0.0017	0.302 ± 0.050	272 ± 11	268 ± 44	98.7	0.62
WC ss-1.21	0.0411 ± 0.0012	0.299 ± 0.032	259.6 ± 7.4	265 ± 28	102.2	1.12
WC ss-1.22	0.0446 ± 0.0015	0.314 ± 0.042	281.0 ± 9.2	278 ± 37	98.8	0.56
WC ss-1.23	0.0439 ± 0.0014	0.304 ± 0.041	276.9 ± 8.7	270 ± 36	97.4	0.66
WC ss-1.24	0.03997 ± 0.00094	0.293 ± 0.026	252.7 ± 6.0	261 ± 23	103.1	0.98
WC ss-1.25	0.0445 ± 0.0014	0.310 ± 0.043	280.7 ± 9.0	274 ± 38	97.7	0.67
WC ss-1.26	0.04308 ± 0.00098	0.293 ± 0.025	271.9 ± 6.2	261 ± 22	96.0	0.53
WC ss-1.27	0.0433 ± 0.0012	0.318 ± 0.036	273.4 ± 7.8	280 ± 32	102.5	0.58
WC ss-1.28	0.0400 ± 0.0013	0.317 ± 0.042	252.9 ± 8.3	280 ± 37	110.5	0.59
WC ss-1.29	0.0439 ± 0.0013	0.308 ± 0.037	276.9 ± 8.1	273 ± 33	98.5	0.63
WC ss-1.30	0.03990 ± 0.00086	0.290 ± 0.020	252.2 ± 5.4	259 ± 18	102.6	1.39
WC ss-1.31	0.0409 ± 0.0014	0.277 ± 0.042	258.3 ± 9.0	249 ± 38	96.3	0.55
WC ss-1.32	*0.0404 ± 0.0013*	*0.327 ± 0.042*	*255.3 ± 8.3*	*287 ± 37*	*112.4*	*0.69*
WC ss-1.33	*0.0398 ± 0.0013*	*0.330 ± 0.042*	*251.7 ± 8.2*	*290 ± 37*	*115.1*	*0.89*
WC ss-1.34	0.0427 ± 0.0014	0.307 ± 0.040	269.6 ± 8.6	272 ± 36	100.7	0.62
WC ss-1.35	0.0434 ± 0.0012	0.339 ± 0.036	273.8 ± 7.6	296 ± 31	108.2	0.86
WC ss-1.36	0.0425 ± 0.0011	0.332 ± 0.031	268.5 ± 6.9	291 ± 27	108.3	0.71
WC ss-1.37	0.0453 ± 0.0014	0.343 ± 0.042	285.5 ± 8.8	300 ± 37	104.9	0.56
WC ss-1.38	0.0423 ± 0.0011	0.281 ± 0.029	266.9 ± 7.0	252 ± 26	94.2	0.86
WC ss-1.39	0.0467 ± 0.0013	0.309 ± 0.034	294.4 ± 8.0	273 ± 30	92.9	0.83
WC ss-1.40	0.0409 ± 0.0013	0.289 ± 0.039	258.5 ± 8.3	258 ± 35	99.7	0.66
WC ss-1.41	0.0404 ± 0.0012	0.296 ± 0.035	255.2 ± 7.5	263 ± 31	103.1	0.53
WC ss-1.42	0.0477 ± 0.0011	0.353 ± 0.031	300.3 ± 7.2	307 ± 27	102.2	0.70
WC ss-1.43	0.0452 ± 0.0013	0.329 ± 0.036	285.0 ± 7.9	289 ± 31	101.3	0.96
WC ss-1.44	0.0445 ± 0.0013	0.308 ± 0.025	280.8 ± 8.4	272 ± 22	97.0	0.63

TABLE 1. (*Continued*)

Grain	$^{206}Pb/^{238}U$	$^{207}Pb/^{235}U$	$^{206}Pb/^{238}U$ age (Ma)	$^{207}Pb/^{235}U$ age (Ma)	% conc	Th/U
WC ss-1.45	0.0416 ± 0.0018	0.286 ± 0.049	263 ± 12	255 ± 44	97.3	0.67
WC ss-1.46	0.0406 ± 0.0013	0.294 ± 0.025	256.5 ± 7.9	262 ± 23	102.1	0.63
WC ss-1.47	0.0430 ± 0.0016	0.296 ± 0.040	272 ± 10	263 ± 36	96.9	0.57
WC ss-1.48	0.0422 ± 0.0016	0.316 ± 0.040	266.1 ± 9.9	279 ± 35	104.7	0.59
WC ss-1.49	0.0430 ± 0.0016	0.296 ± 0.040	271 ± 11	284 ± 43	104.8	0.57
WC ss-1.50	0.0430 ± 0.0021	0.327 ± 0.042	271 ± 13	287 ± 37	105.8	0.62
WC ss-1.51	0.0439 ± 0.0021	0.326 ± 0.039	277 ± 13	287 ± 34	103.7	0.78
WC ss-1.52	0.0414 ± 0.0020	0.300 ± 0.039	261 ± 13	266 ± 35	102.0	0.40
WC ss-1.53	0.0440 ± 0.0021	0.301 ± 0.036	278 ± 13	267 ± 32	96.4	0.51
WC ss-1.54	0.0445 ± 0.0023	0.337 ± 0.052	281 ± 15	295 ± 45	105.2	0.72
WC ss-1.55	0.0405 ± 0.0012	0.295 ± 0.026	255.8 ± 7.6	262 ± 24	102.6	1.03
WC ss-1.56	0.0439 ± 0.0020	0.334 ± 0.060	277 ± 12	293 ± 52	105.6	0.46
WC ss-1.57	0.0468 ± 0.0014	0.332 ± 0.030	294.6 ± 8.7	291 ± 26	98.9	1.14
WC ss-1.58	0.0426 ± 0.0017	0.285 ± 0.044	269 ± 11	254 ± 40	94.5	0.64
WC ss-1.59	0.0450 ± 0.0016	0.334 ± 0.040	283.8 ± 9.8	292 ± 35	103.0	0.67
WC ss-1.60	0.0457 ± 0.0013	0.309 ± 0.024	288.1 ± 7.9	273 ± 21	94.9	0.53
WC ss-1.61	0.0433 ± 0.0012	0.306 ± 0.025	273.4 ± 7.8	271 ± 22	99.0	0.62
WC ss-1.62	0.0443 ± 0.0012	0.304 ± 0.024	279.3 ± 7.7	269 ± 21	96.4	1.10
WC ss-1.63	0.0409 ± 0.0012	0.324 ± 0.030	258.4 ± 7.8	285 ± 27	110.1	0.96
WC ss-1.64	0.0462 ± 0.0018	0.365 ± 0.052	291 ± 11	316 ± 45	108.4	0.63
WC ss-1.65	0.0458 ± 0.0015	0.342 ± 0.038	288.5 ± 9.5	298 ± 33	103.4	0.69
WC ss-1.66	0.0434 ± 0.0013	0.293 ± 0.027	274.1 ± 8.0	261 ± 24	95.3	0.74
WC ss-1.67	0.0411 ± 0.0014	0.327 ± 0.038	259.4 ± 8.8	288 ± 33	110.9	0.78
WC ss-1.68	0.0393 ± 0.0014	0.277 ± 0.037	248.7 ± 8.9	248 ± 33	99.8	0.62
WC ss-1.69	0.0405 ± 0.0010	0.292 ± 0.015	256.0 ± 6.3	260 ± 14	101.6	0.68
WC ss-1.70	0.0421 ± 0.0014	0.330 ± 0.038	265.8 ± 9.0	289 ± 34	108.9	0.78
WC ss-1.71	0.0440 ± 0.0015	0.283 ± 0.040	277.4 ± 9.7	253 ± 35	91.1	0.63
WC ss-1.72	0.0420 ± 0.0012	0.310 ± 0.030	265.5 ± 7.7	274 ± 26	103.2	0.94
WC ss-1.73	0.0421 ± 0.0014	0.302 ± 0.035	265.8 ± 8.6	268 ± 31	101.0	1.06
WC ss-1.74	0.0434 ± 0.0013	0.347 ± 0.034	274.1 ± 8.2	302 ± 30	110.3	0.67
WC ss-1.75	0.0460 ± 0.0015	0.336 ± 0.040	289.7 ± 9.4	294 ± 35	101.6	0.71
WC ss-1.76	0.0416 ± 0.0011	0.297 ± 0.025	262.5 ± 7.2	264 ± 22	100.5	0.53
WC ss-1.77	0.0427 ± 0.0015	0.313 ± 0.039	269.7 ± 9.2	276 ± 35	102.4	0.77
Ashidani Formation: Sandstone (12111007; N35°53'21.57", E136°40'48.82")						
AS-1.1	0.0462 ± 0.0015	0.324 ± 0.039	290.9 ± 9.5	285 ± 34	102.2	0.93
AS-1.2	0.0491 ± 0.0016	0.387 ± 0.045	309 ± 10	332 ± 39	93.1	0.66
AS-1.3	0.0426 ± 0.0018	0.279 ± 0.051	269 ± 11	250 ± 46	107.7	0.65
AS-1.4	0.0486 ± 0.0016	0.355 ± 0.043	306 ± 10	309 ± 37	99.1	0.78
AS-1.5	*0.0449 ± 0.0014*	*0.477 ± 0.045*	*283.1 ± 8.8*	*396 ± 37*	*71.5*	*1.2*
AS-1.6	0.0433 ± 0.0018	0.289 ± 0.053	273 ± 12	257 ± 47	106.2	0.75
AS-1.7	*0.0405 ± 0.0015*	*0.368 ± 0.047*	*255.7 ± 9.4*	*318 ± 40*	*80.4*	*0.96*
AS-1.8	0.0417 ± 0.0015	0.305 ± 0.040	263.1 ± 9.3	270 ± 35	97.3	0.74
AS-1.9	*0.0438 ± 0.0018*	*0.845 ± 0.096*	*277 ± 11*	*622 ± 71*	*44.5*	*0.78*
AS-1.10	0.0413 ± 0.0012	0.330 ± 0.034	260.9 ± 7.3	289 ± 30	90.2	1.2
AS-1.11	0.0411 ± 0.0015	0.315 ± 0.046	259.5 ± 9.3	278 ± 40	93.4	0.94
AS-1.12	0.0451 ± 0.0012	0.331 ± 0.035	284.4 ± 7.8	290 ± 30	98.1	0.71
AS-1.13	0.04379 ± 0.00090	0.315 ± 0.021	276.3 ± 5.7	278 ± 18	99.3	0.74
AS-1.14	0.0414 ± 0.0011	0.309 ± 0.030	261.5 ± 6.9	273 ± 27	95.8	1.0
AS-1.15	0.0436 ± 0.0012	0.335 ± 0.031	275.1 ± 7.4	294 ± 27	93.7	0.64
AS-1.16	0.0430 ± 0.0010	0.337 ± 0.024	271.2 ± 6.5	295 ± 21	92.0	0.63
AS-1.17	0.0440 ± 0.0012	0.325 ± 0.031	277.3 ± 7.5	286 ± 27	97.0	0.65
AS-1.18	0.0483 ± 0.0013	0.349 ± 0.034	303.8 ± 8.3	304 ± 30	100.0	0.73
AS-1.19	*0.0455 ± 0.0011*	*0.291 ± 0.025*	*286.6 ± 7.1*	*259 ± 22*	*110.6*	*1.0*
AS-1.20	0.0447 ± 0.0018	0.303 ± 0.054	282 ± 12	269 ± 48	104.9	0.59
AS-1.21	*0.0453 ± 0.0013*	*0.388 ± 0.038*	*285.7 ± 8.2*	*333 ± 32*	*85.9*	*0.65*
AS-1.22	0.0431 ± 0.0016	0.344 ± 0.052	272 ± 10	300 ± 46	90.5	0.37
AS-1.23	0.04324 ± 0.00094	0.306 ± 0.028	272.9 ± 5.9	271 ± 25	100.6	0.68
AS-1.24	0.0427 ± 0.0010	0.329 ± 0.032	269.2 ± 6.3	289 ± 28	93.1	0.49
AS-1.25	*0.0441 ± 0.0010*	*0.282 ± 0.028*	*277.9 ± 6.1*	*252 ± 25*	*110.3*	*0.61*
AS-1.26	0.0424 ± 0.0013	0.288 ± 0.042	267.9 ± 8.5	257 ± 37	104.3	0.60
AS-1.27	0.04346 ± 0.00095	0.332 ± 0.030	274.2 ± 6.0	291 ± 26	94.3	1.1
AS-1.28	0.04289 ± 0.00086	0.309 ± 0.026	270.7 ± 5.4	274 ± 23	99.0	0.75
AS-1.29	0.0433 ± 0.0012	0.312 ± 0.037	273.0 ± 7.5	276 ± 33	99.1	0.86
AS-1.30	0.0484 ± 0.0014	0.335 ± 0.043	304.8 ± 8.7	293 ± 38	103.9	0.78
AS-1.31	*0.0415 ± 0.0020*	*0.362 ± 0.054*	*262 ± 12*	*314 ± 47*	*83.6*	*0.82*
AS-1.32	*0.0346 ± 0.0016*	*0.789 ± 0.078*	*219 ± 10*	*591 ± 58*	*37.2*	*0.70*
AS-1.33	0.0442 ± 0.0016	0.314 ± 0.027	279 ± 10	277 ± 24	100.5	1.6
AS-1.34	0.0490 ± 0.0023	0.348 ± 0.055	309 ± 14	303 ± 48	101.7	0.76
AS-1.35	0.0433 ± 0.0016	0.341 ± 0.028	274 ± 10	298 ± 24	91.9	1.2
AS-1.36	0.0411 ± 0.0015	0.291 ± 0.026	259.3 ± 9.6	259 ± 23	100.0	1.2
AS-1.37	*0.0407 ± 0.0018*	*0.362 ± 0.047*	*257 ± 11*	*314 ± 41*	*82.0*	*1.0*
AS-1.38	*0.0412 ± 0.0020*	*0.352 ± 0.061*	*261 ± 13*	*306 ± 53*	*85.1*	*0.70*
AS-1.39	0.0423 ± 0.0017	0.329 ± 0.043	267 ± 10	289 ± 38	92.5	0.76
AS-1.40	0.0428 ± 0.0015	0.319 ± 0.036	270.3 ± 9.8	281 ± 32	96.3	0.52
AS-1.41	*0.0440 ± 0.0018*	*0.367 ± 0.050*	*278 ± 11*	*317 ± 43*	*87.5*	*0.61*
AS-1.42	*0.0427 ± 0.0018*	*0.253 ± 0.042*	*270 ± 11*	*229 ± 38*	*117.7*	*0.82*
AS-1.43	0.0430 ± 0.0021	0.336 ± 0.063	272 ± 13	294 ± 55	92.2	0.80
AS-1.44	0.0421 ± 0.0012	0.309 ± 0.019	265.6 ± 7.8	273 ± 17	97.2	0.44
AS-1.45	0.0421 ± 0.0013	0.301 ± 0.022	265.7 ± 8.1	267 ± 19	99.3	1.3
AS-1.46	0.0446 ± 0.0018	0.333 ± 0.048	281 ± 12	292 ± 42	96.2	0.91

TABLE 1. (*Continued*)

Grain	$^{206}Pb/^{238}U$	$^{207}Pb/^{235}U$	$^{206}Pb/^{238}U$ age (Ma)	$^{207}Pb/^{235}U$ age (Ma)	% conc	Th/U
Otani Formation: Sandstone (12111003; N35°52'49.18", E136°43'39.54")						
OT-1.1	0.0386 ± 0.0014	0.291 ± 0.038	244.2 ± 9.1	259 ± 34	94.3	0.44
OT-1.2	0.0375 ± 0.0015	0.280 ± 0.039	237.3 ± 9.3	251 ± 35	94.7	0.81
OT-1.3	0.0798 ± 0.0026	0.562 ± 0.058	495 ± 16	453 ± 47	109.3	0.65
OT-1.4	0.0410 ± 0.0029	0.31 ± 0.10	259 ± 18	271 ± 91	95.5	0.55
OT-1.5	0.3056 ± 0.0086	4.71 ± 0.23	1719 ± 48	1768 ± 87	97.2	0.31
OT-1.6	0.0392 ± 0.0016	0.255 ± 0.040	248 ± 10	231 ± 36	107.3	0.78
OT-1.7	0.0753 ± 0.0027	0.549 ± 0.063	468 ± 17	444 ± 51	105.3	0.54
OT-1.8	0.0427 ± 0.0016	0.284 ± 0.038	269 ± 10	254 ± 34	106.3	0.90
OT-1.9	0.0693 ± 0.0017	0.577 ± 0.047	432 ± 10	462 ± 38	93.4	0.46
OT-1.10	0.0794 ± 0.0020	0.610 ± 0.055	493 ± 12	483 ± 43	101.9	0.54
OT-1.11	0.0401 ± 0.0023	0.296 ± 0.087	254 ± 14	263 ± 78	96.3	0.44
OT-1.12	0.0702 ± 0.0019	0.564 ± 0.055	438 ± 12	454 ± 44	96.4	0.47
OT-1.13	0.4538 ± 0.0075	10.36 ± 0.32	2412 ± 40	2467 ± 75	97.8	0.26
OT-1.14	*0.0389 ± 0.0019*	*0.239 ± 0.065*	*246 ± 12*	*217 ± 59*	*113.1*	*0.48*
OT-1.15	0.0383 ± 0.0015	0.285 ± 0.050	242.1 ± 9.4	255 ± 45	95.0	0.65
OT-1.16	0.03831 ± 0.00090	0.275 ± 0.023	242.4 ± 5.7	247 ± 21	98.2	1.3
OT-1.17	0.0840 ± 0.0051	0.61 ± 0.20	520 ± 32	480 ± 159	108.2	0.34
Hayama Formation: Sandstone (Sample 13042802; N34°47'58.4", E133°30'45.8")						
HY-1.1	0.0438 ± 0.0011	0.289 ± 0.022	276.1 ± 7.1	258 ± 19	107.1	0.56
HY-1.2	*0.0433 ± 0.0014*	*0.383 ± 0.040*	*273.4 ± 8.7*	*329 ± 34*	*83.1*	*0.45*
HY-1.3	0.0428 ± 0.0012	0.303 ± 0.027	270.4 ± 7.5	269 ± 24	100.7	0.46
HY-1.4	*0.0456 ± 0.0013*	*0.386 ± 0.032*	*287.7 ± 8.1*	*331 ± 28*	*86.8*	*0.66*
HY-1.5	0.0431 ± 0.0011	0.336 ± 0.022	271.9 ± 6.9	294 ± 19	92.5	0.85
HY-1.6	0.0499 ± 0.0020	0.390 ± 0.063	314 ± 13	334 ± 54	93.9	0.59
HY-1.7	0.0484 ± 0.0018	0.376 ± 0.054	304 ± 12	324 ± 46	93.9	0.61
HY-1.8	*0.0459 ± 0.0015*	*0.453 ± 0.048*	*289.4 ± 9.7*	*379 ± 40*	*76.3*	*0.83*
HY-1.9	0.0449 ± 0.0014	0.337 ± 0.037	283.4 ± 9.0	295 ± 32	96.1	0.47
HY-1.10	0.0431 ± 0.0013	0.316 ± 0.031	271.9 ± 8.2	278 ± 28	97.7	0.83
HY-1.11	0.0903 ± 0.0026	0.829 ± 0.067	557 ± 16	613 ± 49	90.9	0.13
HY-1.12	0.03195 ± 0.00075	0.223 ± 0.019	202.8 ± 4.8	205 ± 18	99.1	0.88
HY-1.13	0.0471 ± 0.0010	0.325 ± 0.023	296.6 ± 6.5	286 ± 20	103.7	0.79
HY-1.14	0.0454 ± 0.0015	0.340 ± 0.061	286.5 ± 9.4	297 ± 53	96.4	0.21
HY-1.15	*0.0426 ± 0.0014*	*0.351 ± 0.057*	*268.9 ± 8.7*	*306 ± 49*	*88.0*	*0.60*
HY-1.16	0.0466 ± 0.0014	0.331 ± 0.051	293.7 ± 8.9	290 ± 45	101.3	0.76
HY-1.17	0.0443 ± 0.0017	0.352 ± 0.051	279 ± 11	306 ± 44	91.3	0.56
HY-1.18	*0.0584 ± 0.0025*	*0.517 ± 0.081*	*366 ± 15*	*423 ± 66*	*86.6*	*0.62*
HY-1.19	0.0439 ± 0.0011	0.313 ± 0.022	276.8 ± 7.0	277 ± 20	100.0	0.64
HY-1.20	*0.0803 ± 0.0022*	*0.542 ± 0.048*	*498 ± 14*	*440 ± 39*	*113.2*	*0.55*
HY-1.21	0.2688 ± 0.0061	3.453 ± 0.146	1535 ± 35	1516 ± 64	101.2	0.40
HY-1.22	0.01782 ± 0.00054	0.130 ± 0.014	113.9 ± 3.5	124 ± 13	91.9	0.99
HY-1.23	*0.01754 ± 0.00086*	*0.133 ± 0.027*	*112.1 ± 5.5*	*127 ± 26*	*88.3*	*0.72*
HY-1.24	0.01627 ± 0.00048	0.101 ± 0.013	104.1 ± 3.1	97 ± 13	106.8	0.60
HY-1.25	0.03922 ± 0.00077	0.286 ± 0.020	248.0 ± 4.9	255 ± 18	97.2	0.78
HY-1.26	0.05145 ± 0.00097	0.406 ± 0.025	323.4 ± 6.1	346 ± 21	93.4	0.45
HY-1.27	0.04051 ± 0.00083	0.310 ± 0.022	256.0 ± 5.2	274 ± 20	93.5	0.80
HY-1.28	*0.0466 ± 0.0013*	*0.420 ± 0.044*	*293.6 ± 8.4*	*356 ± 38*	*82.5*	*0.46*
HY-1.29	0.04415 ± 0.00064	0.3308 ± 0.0098	278.5 ± 4.0	290.2 ± 8.6	96.0	0.80
HY-1.30	0.0526 ± 0.0019	0.410 ± 0.025	331 ± 12	349 ± 21	94.7	1.70
HY-1.31	0.0442 ± 0.0017	0.314 ± 0.028	279 ± 11	277 ± 25	100.4	0.50
HY-1.32	0.0494 ± 0.0019	0.384 ± 0.033	311 ± 12	330 ± 28	94.2	0.58
HY-1.33	*0.0405 ± 0.0017*	*0.457 ± 0.049*	*256 ± 11*	*382 ± 41*	*66.9*	*0.44*
HY-1.34	*0.0447 ± 0.0020*	*0.266 ± 0.042*	*282 ± 13*	*240 ± 38*	*117.7*	*0.43*
HY-1.35	0.0452 ± 0.0017	0.332 ± 0.028	285 ± 11	291 ± 24	98.0	0.71
HY-1.36	0.0315 ± 0.0015	0.211 ± 0.035	199.9 ± 9.5	194 ± 33	102.8	0.60
HY-1.37	0.0518 ± 0.0021	0.384 ± 0.043	325 ± 13	330 ± 37	98.6	0.95
HY-1.38	0.0443 ± 0.0014	0.307 ± 0.028	279.3 ± 8.6	271 ± 24	102.9	0.61
HY-1.39	0.0848 ± 0.0040	0.69 ± 0.12	524 ± 25	532 ± 94	98.6	0.43
HY-1.40	0.0805 ± 0.0022	0.634 ± 0.036	499 ± 14	499 ± 29	100.1	0.49
HY-1.41	0.0522 ± 0.0019	0.374 ± 0.047	328 ± 12	323 ± 41	101.7	0.57
HY-1.42	0.0427 ± 0.0020	0.310 ± 0.044	270 ± 12	274 ± 39	98.4	0.72
HY-1.43	0.0447 ± 0.0017	0.329 ± 0.022	282 ± 11	289 ± 20	97.6	0.72
HY-1.44	*0.0399 ± 0.0015*	*0.322 ± 0.025*	*252.5 ± 9.7*	*283 ± 22*	*89.2*	*0.74*
HY-1.45	0.0419 ± 0.0020	0.307 ± 0.048	265 ± 13	272 ± 43	97.3	0.52
HY-1.46	0.0405 ± 0.0015	0.302 ± 0.020	255.8 ± 9.5	268 ± 18	95.4	0.63
HY-1.47	0.0441 ± 0.0018	0.343 ± 0.031	278 ± 11	299 ± 27	93.0	0.31
HY-1.48	0.01715 ± 0.00079	0.123 ± 0.017	109.6 ± 5.0	118 ± 17	93.0	1.11

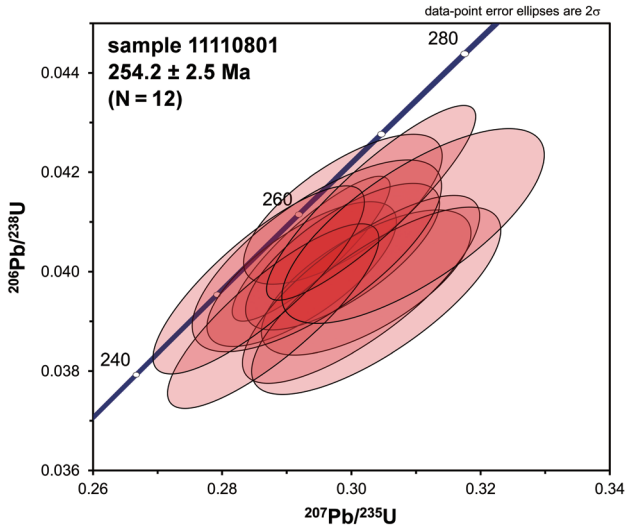

FIGURE 4. Concordia diagram for all the analytical data of detrital zircons from volcaniclastic conglomerate of the Nakajima Tuff Breccia Member of the Motodo Formation (sample 11110801). Abbreviation (Figs. 4–10)—N: total number of analyses.

Andesitic volcaniclastic conglomerate of the Nakajima Tuff Breccia Member (Sample 11110801)

We obtained, in ERI, 12 analyses from 12 zircon grains collected from sample 11110801 of the andesitic volcaniclastic conglomerate of the Nakajima Tuff Breccia Member, Motodo Formation. All the data were concordant, with the % conc value (100•(^{207}Pb/^{235}U age)/(^{206}Pb/^{238}U age)) between 90 and 110. The ^{206}Pb/^{238}U ages of the zircons all fell between 247 Ma and 261 Ma (best estimate ages; Fig. 4) and their weighted mean was 254.2 ± 2.5 Ma (2σ). The Th/U ratio of each analysis was 0.44–2.43 and fell in the range of igneous zircon, Th/U>0.1 (Rubatto and Hermann, 2003).

Andesitic tuff breccia of the Nakajima Tuff Breccia Member (Sample 12082601)

We obtained, in ERI, 14 analyses from 14 zircon grains collected from sample 12082601 of the andesitic tuff breccia of the Nakajima Tuff Breccia Member, Motodo Formation. All the data except one were concordant, with the % conc value between 90 and 110. The ^{206}Pb/^{238}U ages of the concordant zircons all fell between 248 Ma and 281 Ma (best estimate ages; Fig. 5a) and their weighted mean was 269.4 ± 6.2 Ma. The Th/U ratio of each analysis was 0.40–1.05 and fell in the range of igneous zircon. We interpreted that the zircons were divided into two age groups on the concordia diagram and the older group (10 grains) consisted of inherited or exotic zircons. We calculated the concordia age of the younger group (3 grains); that was 253.0 ± 3.6 Ma (Fig. 5b).

Granodiorite cobble of the Wasadani Conglomerate Member (Sample 12082602)

We obtained, in ERI, 14 analyses from 14 zircon grains collected from sample 12082602 of the granodiorite cobble of the Wasadani Conglomerate Member, Motodo Formation. All the data except two were concordant, with the % conc value between 90 and 110 (Table 1). The ^{206}Pb/^{238}U ages of the concordant zircons all fell between 243 Ma and 264 Ma (best estimate ages; Fig. 6) and their weighted mean was 252.6 ± 3.6 Ma. The concordant age of the youngest zircon was 245.1 ± 5.9 Ma. The Th/U ratio of each analysis was 1.00–1.53 and fell in the range of igneous zircon.

Sandstone of the Wasadani Conglomerate Member (Sample 12082603)

We obtained, in NU, 77 analyses from 77 zircon grains collected from sandstone sample 12082603 of the Wasadani Conglomerate Member. Detrital zircons formed a single cluster on the concordia diagram at 308–248 Ma (Fig. 7a). We further chose 74 concordant grains and drew a probability density plot (Fig. 7b). The histogram of course showed a unimodal pattern with the youngest concordant age of 248.7 ± 8.8 Ma and %Pc (percentage of Precambrian zircons) of 0. The peak on the probability density plot was 271 Ma. The Th/U ratio of each analysis was 0.40–1.64 and fell in the range of igneous zircon.

Sandstone of the Ashidani Formation (Sample 12111007)

We obtained 46 analyses from 46 zircon grains collected from sample 12111007 of the Ashidani Formation in NU. Detrital zircons formed a single cluster on the concordia diagram at 320–245 Ma (Fig. 8a). We further chose 34 concordant grains and drew a probability density plot and a histogram with the data interval of 50 Myr (^{206}Pb/^{238}U age; Fig. 8b). The diagrams showed a unimodal pattern with the youngest concordant age of 259.3 ± 9.4 Ma and %Pc of 0. The youngest peak on the probability density plot was 272 Ma. The Th/U ratio of each analysis was 0.37–1.60 and fell in the range of igneous zircon.

Sandstone of the Otani Formation (Sample 12111003)

We obtained 17 analyses from 17 zircon grains collected from sample 12111003 of the Otani Formation in NU. Detrital zircons formed two clusters and two separate plots on the concordia diagram (Fig. 9a, b): 270–235 Ma (53%), 520–430 Ma (35%), 1719 Ma (6%), and 2412 Ma (6%). We further chose 16 concordant grains and drew a probability density plot and a histogram with the data interval of 50 Myr (^{206}Pb/^{238}U age; Fig. 9c). The histogram showed a quasi-bimodal pattern with the youngest concordant age of 237.4 ± 9.1 Ma and %Pc of 12. The youngest peak in the probability density plot was 243 Ma. The Th/U ratio of each analysis was 0.26–1.30 and fell in the range of igneous zircon.

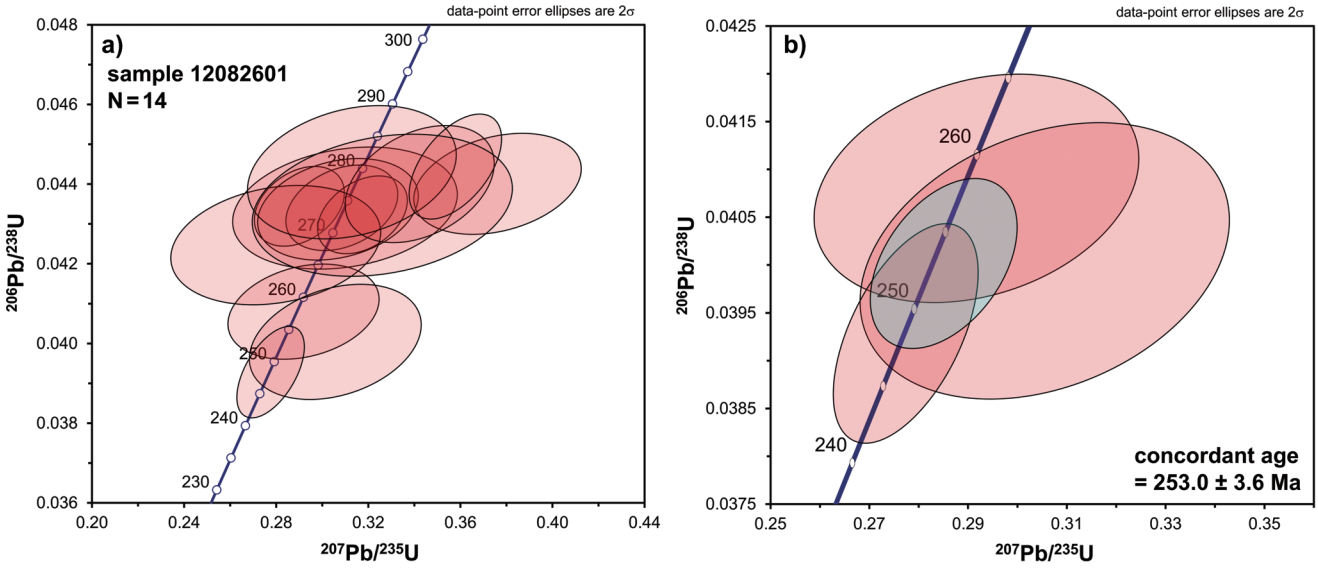

FIGURE 5. Analytical data of detrital zircons from andesitic tuff breccia of the Nakajima Tuff Breccia Member of the Motodo Formation (sample 12082601). **a,** Concordia diagram for all data; **b,** Concordia diagram for 265–240 Ma data set. The gray ellipse denotes the concordant age.

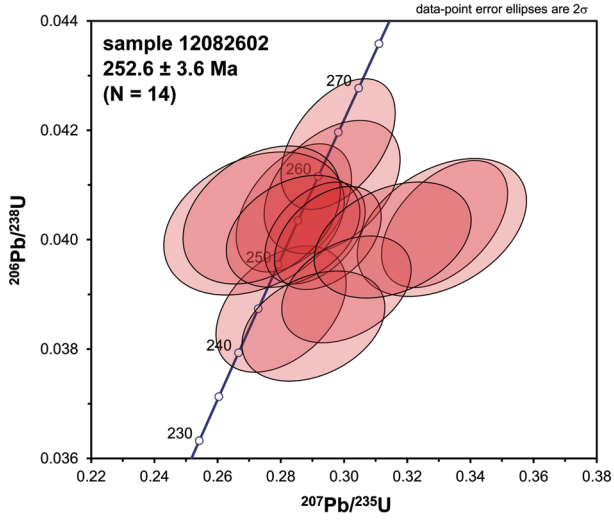

FIGURE 6. Concordia diagram for all the analytical data of detrital zircons from a granodiorite cobble of the Wasadani Conglomerate Member of the Motodo Formation (sample 12082602).

Sandstone of the Hayama Formation (Sample 13042802)

We obtained 48 analyses from 48 zircon grains collected from sample 13042802 of the Hayama Formation in NU. Detrital zircons formed one cluster and four separate concordant plots on the concordia diagram (Fig. 10a, b). The cluster is 348–248 Ma (80%), whereas the separate concordant plots are at 114–104 Ma (6%), 203 Ma (6%), 557 Ma (6%), and 1535 Ma (2%). We further chose 37 concordant grains and drew a probability density plot and a histogram with the data interval of 50 Myr ($^{206}Pb/^{238}U$ age; Fig. 10c). The histogram showed a multimodal pattern with the youngest concordant age of 113.8 ± 3.4 Ma and %Pc of 8. The youngest peak on the probability density plot was 104 Ma. The Th/U ratio of each analysis was 0.26–1.30 and fell in the range of igneous zircon.

DISCUSSION

Age of deposition of the Motodo Formation

Although most of the previous studies suggested that the Motodo Formation is correlated with the Early Cretaceous Kenseki Formation or Kanmon Group (e.g., Kobayashi, 1954; Kawai et al., 1957; Ono et al., 2003; Matsumoto, 2012b), our data do not support the idea. Considering the pyroclastic or volcaniclastic nature of the Nakajima Tuff Breccia Member, the hinterland must have been an active volcanic terrain that probably supplied syn-sedimentary zircons. The two samples of the Nakajima Tuff Breccia Member we studied, have a single or younger age cluster at 254.2 ± 2.5 Ma (Sample 11110801) and 253.0 ± 3.6 Ma (Sample 12082601), strongly suggesting that the member is a product of a Late Permian volcanic activity (252.17–259.8 Ma; International Commission on Stratigraphy, 2013).

The $^{206}Pb/^{238}U$ ages of the concordant zircons from the granodiorite cobble of the Wasadani Conglomerate Member all fell between 243 Ma and 264 Ma, with the weighted mean of 252.6±3.6 Ma. The data indicate that the granodiorite was crystallized in end Permian and was later supplied to the depositional site of the Wasadani Conglomerate Member. The detrital zircon ages of the matrix sandstone of the member

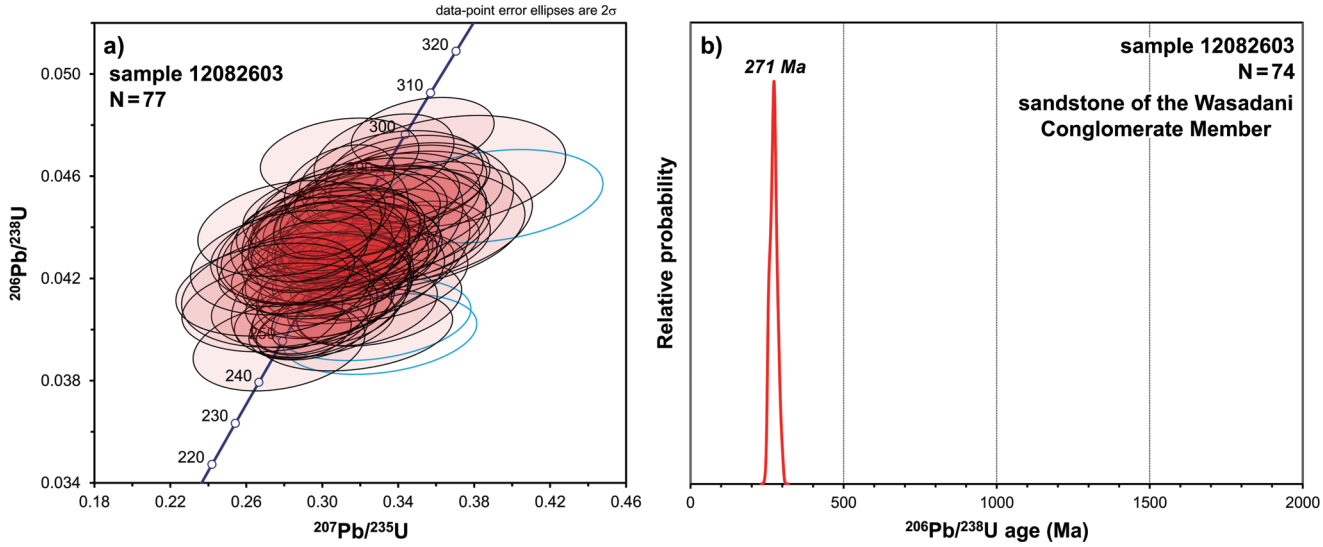

FIGURE 7. Analytical data of detrital zircons from sandstone of the Wasadani Conglomerate Member of the Motodo Formation (sample 12082603). **a,** Concordia diagram for all data; **b,** Probability density plot. Open (blue) circles in the concordia diagrams from Fig. 7 to Fig. 10 show the analytical data for discordant grains.

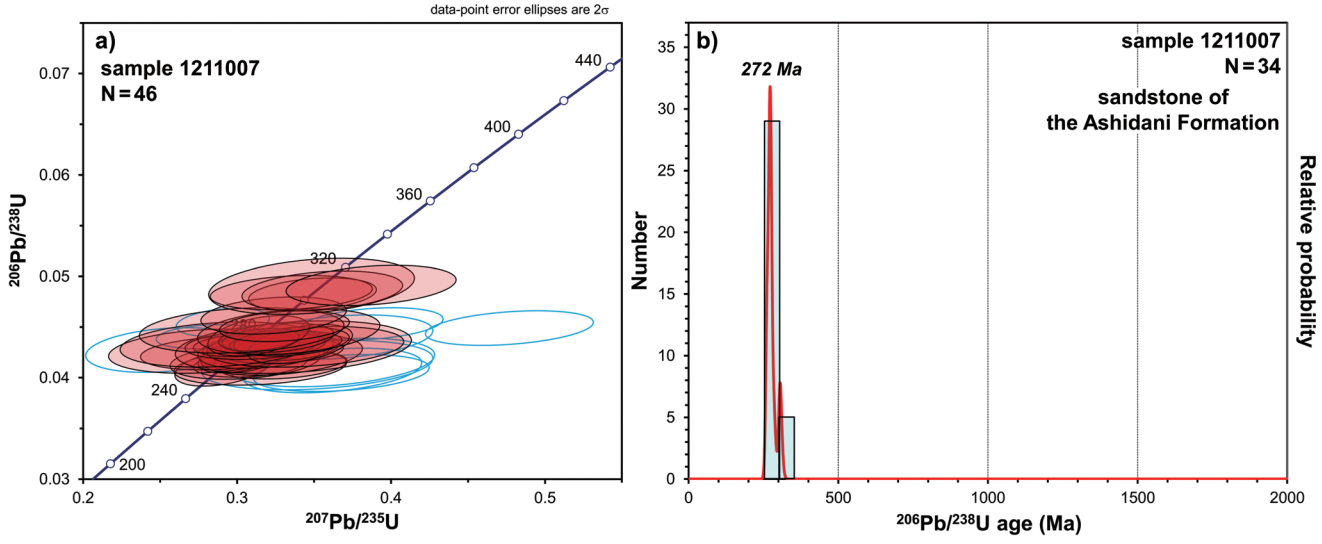

FIGURE 8. Analytical data of detrital zircons from sandstone of the Ashidani Formation (sample 12111007). **a,** Concordia diagram for all data; **b,** Probability density plot with histogram.

make a single age cluster between 248 Ma and 308 Ma, with a single peak in the probability density plot at 271 Ma. These geochronological data from the Wasadani Conglomerate Member indicate that the member is of Late Permian–Early Triassic age or younger. However, considering the fact that the Wasadani Conglomerate Member conformably covers the Nakajima Tuff Breccia Member (Ono and Takeuchi, 2001) and the latter member is a product of Late Permian volcanism in the hinterland, we conclude that the Wasadani Conglomerate Member is correlated with the Upper Permian–Lower Triassic.

Ono et al. (2003) reported CHIME zircon ages of 201 ± 20 Ma and 202 ± 30 Ma from granodiorite clasts of the Wasadani Conglomerate Member. According to the paper, however, the isochron of 201 ± 20 Ma was strongly influenced by a couple of spots with high UO_2 content that were likely on hydrothermally grown parts of the zircons. Considering that (1) some 90 zircons from the Wasadani Conglomerate Member we analyzed were all older than 243 Ma, and (2) the CHIME zircon ages

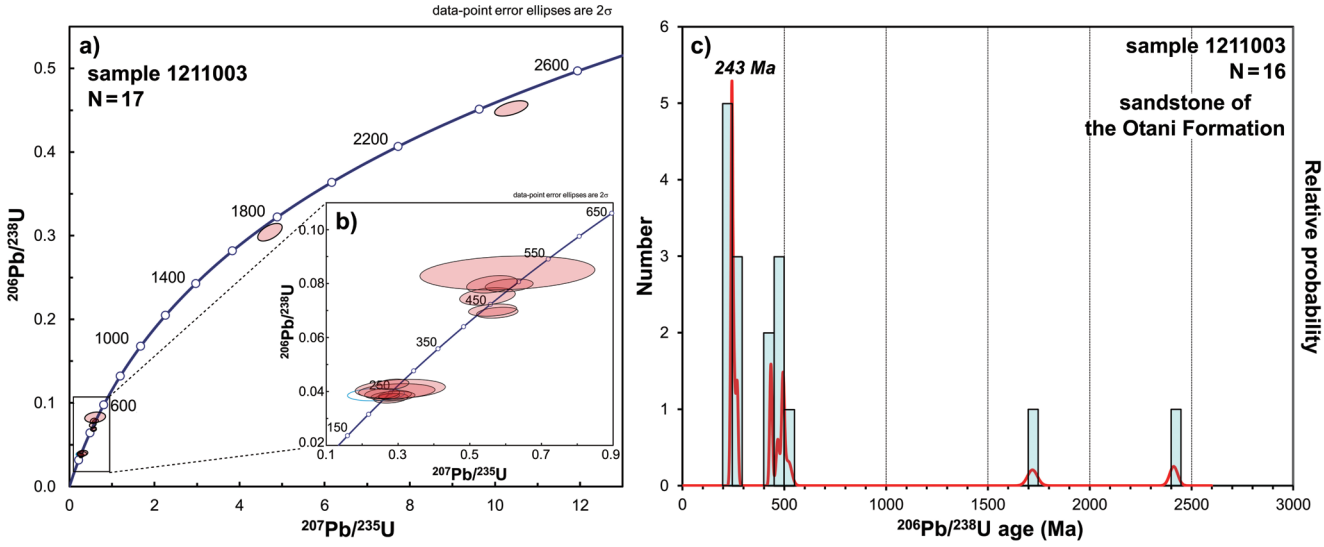

FIGURE 9. Analytical data of detrital zircons from volcaniclastic sandstone of the Otani Formation (sample 12111003). **a,** Concordia diagram for all data; **b,** Concordia diagram for 650–150 Ma data set; **c,** Probability density plot with histogram..

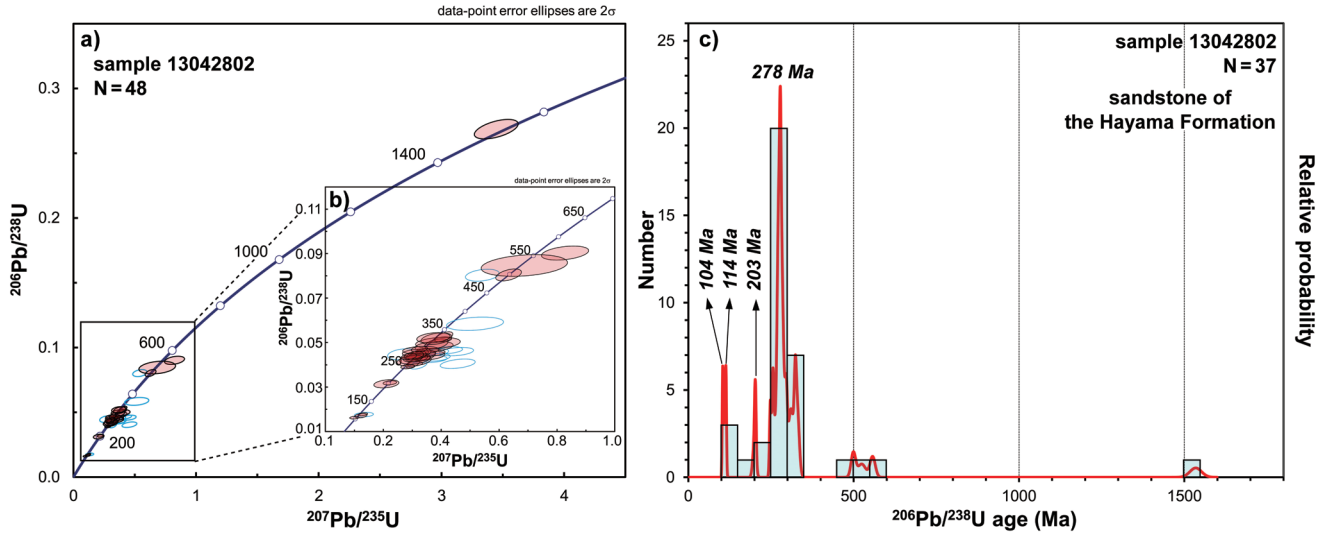

FIGURE 10. Analytical data of detrital zircons from red sandstone of the Hayama Formation (former Kenseki Formation; sample 13042802). **a,** Concordia diagram for all data; **b,** Concordia diagram for 700–100 Ma data set; **c,** Probability density plot with histogram. Note the difference in the detrital zircon age distribution from the sandstone of the Motodo Formation (Fig. 7).

tend to be younger than biostratigraphically constrained ages (e.g., Suzuki et al., 1992), we suggest that CHIME zircon ages should carefully be reexamined and cross checked with the ages obtained from other methods .

Our preliminary study of the Lower Cretaceous Hayama Formation shows some differences in detrital zircon geochronology from the Motodo Formation. Although we analyzed only 37 concordant zircons of the Hayama Formation, they surely include 114–104 Ma (late Aptian–early Albian) and Precambrian zircons besides 348–248 Ma zircons. Among these age clusters, the 348–248 Ma cluster is close to the age cluster of the detrital zircons from the Wasadani Conglomerate Member (sample 12082603; 308–248 Ma). However the presence of Early Cretaceous and Precambrian zircons in the Hayama sandstone is negative evidence for the correlation between the Motodo and Hayama formations.

From these lines of evidence, we strongly suggest that the Motodo Formation is an Upper Permian to Lower Triassic

formation as Omura (1968) first proposed. The Motodo Formation cannot be correlated with the Lower Cretaceous Kanmon Group, although the occurrence of red bed is a common feature.

Age of deposition of the Ashidani Formation

Matsumoto (2012a) already presented from the SHRIMP dating that the age of detrital zircons of the Ashidani Formation clustered at 280–220 Ma and inferred that the Ashidani Formation is of Triassic age. We also showed that the detrital zircons from sample 12111007 of the Ashidani Formation form a single age-cluster at 320–245 Ma on the concordia diagram, with a single peak in the probability density plot at 272 Ma. Our data logically indicate that sample 12111007 of the Ashidani Formation was deposited at 272 Ma or younger and support the idea of Matsumoto (2012a) that the Ashidani Formation is a Triassic formation, although more critical data are needed.

Age of deposition of the Otani Formation

The detrital zircon geochronology of the volcaniclastic sandstone of the Otani Formation indicates that the age of deposition of the formation is the Middle to Late Triassic. The volcaniclastic sandstone of the Otani Formation contains abundant fragments of andesitic volcanic rocks and the clasts of conglomerate of the Otani Formation are mainly of andesite and basalt (Matsumoto, 2012b). Hence we interpret that the hinterland of the Otani Formation must have been an active volcanic terrain that supplied syn-sedimentary zircons. The sample of volcaniclastic sandstone we studied (sample 12111003), has the youngest age cluster at 270–235 Ma, strongly suggesting that the clasts of volcanic rocks in the Otani Formation are products of a Late Permian to early Late Triassic volcanic activity. The youngest concordant age of detrital zircons of 237.4 ± 9.1 Ma or the youngest peak age on the probability density plot of 243 Ma likely indicate the timing of deposition of the Otani Formation in front of an active volcanic terrain. In this way we suggest that the Otani Formation can be correlated with the Middle Triassic.

The whole rock K-Ar age of 159.3 ± 8.0 Ma (Metal Mining Agency of Japan, 1980) is evidence against our conclusion. However, considering the heavy alteration of the Otani Formation and Late Cretaceous thermal history (e.g., Matsumoto, 2012b), we interpret that the K-Ar age indicates an age of alteration or cooling.

Possible changes of tectonic setting of the Hida Gaien Belt in Early–Middle Triassic times

Although the Paleozoic to Triassic geologic units in the Kuzuryu area are mostly bound by faults or shear zones (Otoh et al., 2004; Matsumoto, 2012b) and do not preserve their original succession, our data imply that the tectonic setting of the Hida Gaien Belt may have changed in Early–Middle Triassic times. The age distributions of detrital zircons in the Motodo and Ashidani sandstone are unimodal, with no Precambrian zircons. The unimodal age distribution suggests that the Motodo and Ashidani sandstone was deposited apart from a large continental block, because Precambrian zircons are generally concentrated in the continental crust. Okawa et al. (2013, this volume) found similar sandstones with unimodal zircon age distribution from the Permian–Lower Jurassic formations of the South Kitakami Belt. They interpreted that the Permian–Lower Jurassic formations were deposited along an oceanic island arc. Likewise the Motodo and Ashidani sandstones, probably of Late Permian to Early Triassic age, may have formed in an oceanic-island-arc setting. The Otani sandstone, on the other hand, contains some Paleoproterozoic zircons (1719 Ma, 2412 Ma) along with some younger (520–430 Ma) zircons. The Otani sandstones, probably of Middle Triassic age, may have formed along an active continental margin where Paleoproterozoic basement rocks and 520–430 Ma igneous rocks were exposed and andesitic volcanism was active. The tectonic setting of the Hida Gaien Belt may have changed in Early–Middle Triassic times from an oceanic island arc to an active continental arc.

The present-day Hida Belt is a candidate for the active continental arc behind the Hida Gaien Belt. However we do not accept the idea, because (1) 520–430 Ma igneous rocks are absent in the Hida Belt (Kunugiza and Kaneko, 2001) and (2) the chemical composition of the granitic gravel in the Otani Formaition is significantly differs from that of the Hida Granite (Matsumoto, 2012b).

Comparison of the tectonic setting with the South Kitakami Belt

The South Kitakami Belt records similar tectonic transition with the Hida Gaien Belt, but the age of the transition was different. As stated in the previous section, Okawa et al. (2013, this volume) clarified that the Permian to Lower Jurassic sandstones of the South Kitakami Belt show unimodal age distribution of detrital zircons and interpreted that they were deposited along an oceanic island arc. For example, the Lower Triassic Osawa Formation of the Inai Group has a single age-cluster at 324–243 Ma (Okawa et al., 2013, this volume). Moreover the Inai Group bears some intercalations of red bed in its lower horizons (Horikawa and Yoshida, 2006). These features are common with the coeval Motodo Formation in the Hida Gaien Belt, having a single age-cluster of detrital zircons at 308–248 Ma, and bearing abundant red beds. The Motodo Formation may have deposited in similar climatic and tectonic conditions with the Inai Group.

In the South Kitakami Belt, the oceanic-island-arc setting continued until Early Jurassic times. The unimodal age-distribution of detrital zircons remains up to the Lower Jurassic Shizugawa Group, and the mixture of Paleoproterozoic zircons become evident from Middle Jurassic beds. Thus the tectonic transition of the South Kitakami Belt from an oceanic island arc to a continental arc took place in the Early–Middle Jurassic,

some 70 Myr later than the similar tectonic transition in the Hida Gaien Belt.

Implications of the new evidence for Late Permian–Triassic volcanism

As described in the introduction of this paper, there was no evidence for volcanism between the Middle Permian mafic to intermediate volcanism in the Sorayama Formation (Tsukada et al., 1999; Tsukada and Takahashi, 2000) and Late Triassic felsic to intermediate volcanism in the Tandodani Formation (Tsukada et al., 1997; Tsukada and Niwa, 2005). The Late Permian to Triassic U-Pb ages from the pyroclastic and volcaniclastic rocks of the Motodo and Otani formations suggest, for the first time, that Late Permian to Triassic volcanic activities left impressions to the Hida Gaien Belt. Combining the new evidence and the results of previous studies listed in the introduction, it is concluded that the Hida Gaien Belt holds evidence for continual volcanism of Ordovician to Late Triassic times. During that period of 270-Myr volcanism, significant tectonic transition from an oceanic island arc to the continental arc, or the amalgamation of oceanic island arc to a continental margin, may have taken place in the Early–Middle Triassic.

ACKNOWLEDGMENTS

We would like to express our sincere gratitude to Emeritus Professor Kenji Konishi of Kanazawa University for his encouragement to submit our work to this volume; and to Professor Masaaki Shimizu and Associate Professor Kenji Kashiwagi of the University of Toyama for various discussions and instructions during the course of this study. Critical reviews of the submitted manuscript by Professor Makoto Takeuchi of Nagoya University, Professor Keitaro Kunugiza of the University of Toyama, Emeritus Professor Kenji Konishi, and Dr. Hiroto Ichishima of the Fukui Prefectural Dinosaur Museum are greatly appreciated. This study was supported by the Earthquake Research Institute (University of Tokyo) cooperative research program 2013-G-04, JSPS KAKENHI Grant Number 25400484, and the discretionary budget of the President of the University of Toyama.

REFERENCES

Corfu, F., J. M. Hanchar, P. W. O. Hosikin and P. Kinny. 2003. Atlas of zircon textures; pp. 469–500 *in* J. M. Hanchar and P. W. O. Hoskin (eds.), Zircon, Reviews in Mineralogy and Geochemistry 53. Mineralogical Society of America, Washington, DC.

Fukui Prefecture. 2010. Geological map of Fukui Prefecture and it's explanatory note (2010). Fukui Prefectural Public Corporation of Construction Technology, Fukui, 173 pp.*

Hamada, T. 1959. On the taxonomic position of *Favosites hidensis* and its Devonian age. Japanese Journal of Geology and Geography 30: 201–213.

Horikawa, H., and K. Yoshida. 2006. The sedimentary environment of the basal part of the Lower Triassic Inai Group in the Toyoma area, South Kitakami Terrane, northeast Japan. Journal of the Geological Society of Japan 112: 469–477.**

Igo, H. 1956. On the Carboniferous and Permian of the Fukuji district, Hida Massif, with special reference to the fusulinid zones of the Ichinotani Group. Journal of the Geological Society of Japan 62: 217–240.**

Igo, H., S. Adachi, H. Furutani and H. Nishiyama. 1980. Ordovician fossils first discovered in Japan. Proceedings of the Japan Academy, Series B, 56: 499–503.

International Commission on Stratigraphy. 2013. International chronostratigraphic chart, v2013/01. http://www.stratigraphy.org/ICSchart/ChronostratChart2013-01.pdf.

Isomi, H., and T. Nozawa. 1957. Geological map of Japan, scale 1:50,000, Funatsu sheet and its explanatory text. Geological Survey of Japan, Kawasaki, 43 pp.**

Kamei, T. 1952. The stratigraphy of the Fukuji district, southern part of Hida Mountainland (Study on Paleozoic rocks of Hida 1). Journal of Shinshu University 2: 43–74.

Kato, M. 1959. Some Carboniferous rugose corals from Ichinotani formation, Japan. Journal of the Faculty of Science, Hokkaido University, Series 4, 10: 263–287.

Kato, T. 1913. Report of the volcanic eruption of Mt. Io-dake (Mt. Yake-dake). Report of the Earthquake Investigation Committee 75: 29–73.*

Kawagoe, Y., S. Sano, Y. Orihashi, H. Obara, Y. Kouchi and S. Otoh. 2012. New detrital zircon age data from the Tetori Group in the Mana and Itoshiro areas of Fukui Prefecture, central Japan. Memoir of the Fukui Prefectural Dinosaur Museum 11: 1–18.

Kawai, M. 1956. On the late Mesozoic movement in the western part of Hida Plateau, Part 1. Journal of the Geological Society of Japan 62: 559–573.**

Kawai, M., K. Hirayama and N. Yamada. 1957. Geological Sheet Map "Arashimadake", Scale 1:50,000, and its Explanatory Text. Geological Survey of Japan , 110 pp.**

Kobayashi, M. 1954. Geology of the environs of Nishitani-mura, Ono-gun, Fukui Prefecture. Studies from the Geological and Mineralogical Institute, Tokyo University of Education 3, Memorial volume dedicated to the late Professor Kiyosuke Kawada, 35–43.**

Kouchi, Y., Y. Orihashi, H. Obara, T. Fujimoto, Y. Haruta, K. Tsukada and K. Yamamoto. 2012. U-Pb age dating for a zircon using 213 nm Nd-YAG laser ablation ICP mass spectrometry: An attempt on optimization of the analytical condition to reduce matrix effect. Abstracts for the 59th annual meeting of the Geochemical Society of Japan: 135.*

Kozu, S. 1910. Report of the geological investigation of the Norikura Volcano. Report of the Earthquake Investigation Committee 71, 1–71.*

Kunugiza, K., A. Goto, T. Itaya and K. Yokoyama. 2004. Geological development of the Hida Gaien belt: Constraints from K-Ar ages of high P/T metamorphic rocks and U-Th-Pb EMP ages of granitic rocks affecting contact metamorphism of

serpentinite. Journal of the Geological Society of Japan 110: 580–590.**

Kunugiza, K., and K. Kaneko. 2001. Metamorphic rocks and granites of the eastern Hida Belt, Toyama Prefecture; pp. 137–156 *in* A. Ishiwatari (ed.), Excursion Guidebook of the 108th Annual Meeting of the Geological Society of Japan. Geological Society of Japan.*

Kurihara, T. 2003. Stratigraphy and geologic age of the Middle Paleozoic strata in the Kuzuryu Lake–Upper Ise River area of the Hida-gaien Terrane, central Japan. Journal of the Geological Society of Japan 109: 425–441.**

Kurihara, T. 2004. Silurian and Devonian radiolarian biostratigraphy of the Hida Gaien belt, central Japan. Journal of the Geological Society of Japan 110: 620–639.**

Kusumi, H., N. Yoshimura and S. Katayama. 1965. Geology of the northwestern part in Nariwa-machi, Okayama Prefecture, Japan. Geological Report of Hiroshima University 14: 397–425.**

Ludwig, K. R. 2008. Isoplot 3.70: Geochronological Toolkit for Microsoft Excel. Berkeley Geochronology Center Special Publication 4, 77 pp.

Maeda, S. 1961. Stratigraphy of the Tetori Group in the southern part of the Kuzuryu River, Fukui Prefecture. Journal of the Geological Society of Japan 67: 23–31.**

Matsumoto, T. 2012a. U-Pb ages of detrital zircons from the Ashidani Formation in the Kuzuryu area, the Hida Gaien Belt. Japan Geoscience Union Meeting 2012: SGL44-03.

Matsumoto, T. 2012b. Geology of the Hida Gaien Belt in the upper Kuzuryu-gawa River area in Ono City, Fukui Prefecture, central Japan. Resource Geology 62: 384–407.

Metal Mining Agency of Japan. 1980. Report of the regional geological survey, Hida area I. Agency of Natural Resources and Energy, Tokyo, 183 pp.*

Niko, S., S. Yamakita, S. Otoh, S. Yanai and T. Hamada. 1987. Permian radiolarians from the Mizuyagadani Formation in Fukuji area, Hida Marginal Belt and their significance. Journal of the Geological Society of Japan 93: 431–433.*

Okawa, H., M. Shimojo, Y. Orihashi, K. Yamamoto, T. Hirata, S. Sano, Y. Ishizaki, Y. Kouchi, S. Yanai and S. Otoh. 2013 (this volume). Detrital zircon geochronology of the Silurian–Lower Cretaceous continuous succession of the South Kitakami Belt, Northeast Japan. Memoir of the Fukui Prefectural Dinosaur Museum 12: 35–78.

Omura, A. 1968. Sedimentological study of the Motodo Formation in the vicinity of Nishitani-mura, Ono-gun, Fukui Prefecture, central Japan. Journal of the Geological Society of Japan 74: 217–231.**

Ono, K., and M. Takeuchi. 2001. Sedimentary facies and clast compositions of the Motodo Formation in Hida-gaien Tectonic Zone, Fukui Prefecture, central Japan. Journal of the Geological Society of Japan 107: 481–495.**

Ono, K. M. Takeuchi and K. Suzuki. 2003. CHIME zircon ages of granodiorite clasts from Motodo Formation, Hida-Gaien Belt, central Japan. Journal of the Geological Society of Japan 109: 257–266.

Orihashi, Y., S. Nakai and T. Hirata. 2008. U-Pb age determination for seven standard zircons using inductively coupled plasma-mass spectrometry coupled with frequency quintupled Nd-YAG (λ = 213 nm) laser ablation system: Comparison with LA-ICP-MS zircon analyses with a NIST glass reference material. Resource Geology 58: 101–123.

Otoh, S. 1985. Unconformity between non-metamorphic Paleozoic strata and the Upper Triassic Nariwa Group in the Oga area, Okayama Prefecture. Journal of the Geological Society of Japan 91: 779–786.**

Otoh, S., M. Niwa, K. Tsukada, M. Aoyama and T. Matsumoto. 2004. Outline of the shear zones in the Kuzuryu area, Hida Gaien belt, Fukui Prefecture, central Japan. Journal of the Geological Society of Japan 110: 598–607.**

Rubatto, D., and J. Hermann. 2003. Zircon formation during fluid circulation in eclogites (Monviso, Western Alps): Implications for Zr and Hf budget in subduction zones. Geochimica et Cosmochimica Acta 67: 2173–2187.

Sano, H., Y. Iijima and H. Hattori. 1987. Stratigraphy of the Paleozoic rocks in the Akiyoshi Terrane of the central Chugoku Massif. Journal of the Geological Society of Japan 93: 865–880.**

Suzuki, K., M. Adachi, K. Sango and H. Chiba. 1992. Chemical Th-U-total Pb isochron ages of monazites and zircons from the Hikami Granite and "Siluro–Devonian" clastic rocks in the South Kitakami terrane. Journal of Mineralogy, Petrology and Economic Geology 87: 330–349.**

Suzuki, S., D. K. Asiedu and T. Fujiwara. 2001. Lower Cretaceous fluvial deposits, Hayama Formation, Nariwa area, Okayama Prefecture, Southwest Japan. Journal of the Geological Society of Japan 107: 541–556.**

Tsukada, K. 1997. Stratigraphy and structure of Paleozoic rocks in the Hitoegane area, Kamitakara Village, Gifu Prefecture. Journal of the Geological Society of Japan 103: 658–668.**

Tsukada, K., and T. Koike. 1997. Ordovician conodonts from the Hitoegane area, Kamitakara Village, Gifu Prefecture. Journal of the Geological Society of Japan 103: 171–174.*

Tsukada, K., and K. Niwa. 2005. The Triassic Tandodani Formation in the Hongo area, Hida Gaien belt, central Japan. Journal of Earth and Planetary Sciences, Nagoya University 52: 1–10.

Tsukada, K., and Y. Takahashi. 2000. Redefinition of the Permian strata in the Hida-gaien Tectonic Zone, Fukuji area, Gifu Prefecture, Central Japan. Journal of the Earth and Planetary Science, Nagoya University 47: 1–35.

Tsukada, K., Y. Takahashi and T. Ozawa. 1999. Stratigraphic relationship between the Mizuyagadani and Sorayama Formations, and age of the Sorayama Formation, in the Hida-gaien Tectonic Zone, Kamitakara Village, Gifu Prefecture, central Japan. Journal of the Geological Society of Japan 105: 496–507.**

Tsukada, K., M. Takeuchi and S. Kojima. 2004. Redefinition of the Hida Gaien belt. Journal of the Geological Society of Japan 110: 640–658.**

Tsukada, K., S. Yamakita and T. Koike. 1997. Late Triassic

conodonts from the Hongo area in the Hida Marginal Belt. Journal of the Geological Society of Japan 103: 1175–1178.*

Wiedenbeck, M., P. Allé, F. Corfu, W. L. Griffin, M. Meier, F. Oberli, A. von Quadt, J. C. Roddick and W. Spiegel. 1995. Three natural zircon standards for U-Th-Pb, Lu-Hf, trace element and REE analyses. Geostandards Newsletter 19: 1–23.

Yamada, K. 1967. Stratigraphy and geologic structure of the Paleozoic formations in the upper Kuzuryu River district, Fukui Prefecture, central Japan. Science Reports of Kanazawa University 12: 185–207.

Yamaguchi, R., and Y. Ohta. 1965. Discovery of *Lepidolina kumaensis* Kanmera from the Ohtani conglomerate in the Ise Region, Fukui Prefecture. Journal of the Geological Society of Japan 71: 276–280.**

*： in Japanese
**： in Japanese with English abstract

＜　地名・地層名　＞

Akubaradani Valley …… 悪原谷
Arakigawa Formation …… 荒城川層
Ashidani Formation …… 芦谷層
Eda Conglomerate Member……枝礫岩部層
Fujikuradani Formation …… 藤倉谷層
Fukuji ……福地
Hayama Formation…… 羽山層
Hida Gaien Belt …… 飛騨外縁帯
Hida granitoids …… 飛騨花崗岩類
Hitoegane Formation …… 一重ケ根層
Ichinomata bridge …… 一の又橋
Inai Group …… 稲井層群
Ise Metamorphic Rocks ……伊勢変成岩類
Iwatsubodani Formation…… 岩坪谷層
Kagero Formation …… 影路層
Kamianama Formation …… 上穴馬層
Kanmon Group …… 関門層群
Kenseki Formation…… 硯石層
Konogidani Formation …… 此木谷層
Konogidani Valley …… 此木谷
Kumokawa Conglomerate Member……雲川礫岩部層
Kumokawa River …… 雲川
Kuzuryu Dam…… 九頭竜ダム
Kuzuryu …… 九頭竜
Lake Kuzuryu-ko …… 九頭竜湖
Mizuyagadani Formation…水屋ケ谷層
Motodo Formation…… 本戸層
Mt. Washikuradake…… 鷲鞍岳
Nagano Formation …… 長野層
Nakajima Tuff Breccia Member ……中島凝灰角礫岩部層
Naradani…… 楢谷
Nariwa Town …… 成羽町
Oguradani Formation…… 小椋谷層
Okayama Prefecture …… 岡山県
Osawa Formation …… 大沢層
Otani Formation…… 大谷層
Sasogawa River …… 笹生川
Shibasudani Formation … 子馬巣谷層
Shimagigawa River…… 島木川
Sorayama Formation …… 空山層
South Kitakami Belt …… 南部北上帯
Takahashi City …… 高梁市
Wasadani Conglomerate Member ……早稲谷礫岩部層